

Double balanced homodyne detection

Kouji Nakamura ^{1*}, and Masa-Katsu Fujimoto ^{1†}

*Gravitational-Wave Project Office, Optical and Infrared Astronomy Division,
National Astronomical Observatory of Japan, Mitaka, Tokyo 181-8588, Japan*

(Dated: May 31, 2019)

In the context of the readout scheme for gravitational-wave detectors, the “double balanced homodyne detection” proposed in [K. Nakamura and M.-K. Fujimoto, arXiv:1709.01697.] is discussed, which enables us to measure the expectation values of the photon creation and annihilation operators. Although it has been said that the operator $\hat{b}_\theta := \cos\theta\hat{b}_1 + \sin\theta\hat{b}_2$ can be measured through the homodyne detection in literature, we first show that the expectation value of the operator b_θ cannot be measured as the linear combination of the upper- and lower-sidebands from the output of the balanced homodyne detection, where \hat{b}_1 and \hat{b}_2 are the amplitude and phase quadrature in the two-photon formulation, respectively. On the other hand, it is shown that the above double balanced homodyne detection enables us to measure the expectation value of the operator \hat{b}_θ if we can appropriately prepare the complex amplitude of the coherent state from the local oscillator. It is also shown that the interferometer set up of the eight-port homodyne detection realizes our idea of the double balanced homodyne detection. We also evaluate the noise-spectral density of the gravitational-wave detectors when our double balanced homodyne detection is applied as their readout scheme. Some requirements for the coherent state from the local oscillator to realize the double balanced homodyne detection are also discussed.

I. INTRODUCTION

In 2015, gravitational waves are directly observed by the Laser Interferometer Gravitational-wave Observatory (LIGO) [1]. The first observing run of the Advanced LIGO identified two binary black hole coalescence signals with high statistical significance, GW150914 [2] and GW151226 [3], as well as a less significant candidates LVT151012 [4]. Furthermore, the second observation run of the Advanced LIGO also identified the a black hole coalescence signal GW170104 [5]. From August 1st in 2017, European gravitational-wave telescope Advanced Virgo [9] joined this second observation run and reported a black hole coalescence signal GW [6] with more precise source location. Furthermore, the first observation of gravitational wave from the neutron star binary coalescence was identified as GW170817 [7] and the electromagnetic counter parts are observed [8]. Due to these reports, the gravitational-wave astronomy and the multi-messenger astronomy including gravitational-wave astronomy have finally begun. In addition to the Advanced LIGO and Advanced Virgo, Japanese gravitational-wave telescope KAGRA [10] is also now preparing for the construction of the network of the gravitational-wave detectors to develop the gravitational-wave astronomy. To develop this gravitational-wave astronomy as a more precise science, improvements of the detector sensitivity is necessary. So, it is important to continue the research and development of the science of gravitational-wave detectors together with the source sciences of gravitational waves. This paper is one of results based on such research activities.

The most difficult challenge in building a laser interferometric gravitational-wave detector is isolating the test masses from the rest of the world and keeping the device locked around the correct point of the operation. After the issues of the isolation and the locking have been solved, we can arrive at the fundamental noise that arises from quantum fluctuations in the system. Actually, in Advanced LIGO, at signal frequencies above a couple of hundreds of Hertz, the sensitivity of current detectors is limited by the photon counting noise at the interferometer readout, which is called shot noise [1]. Furthermore, Advanced Virgo and KAGRA are also expected to be operated in a regime where the quantum physics of both light and mirror motion couple to each other. To achieve sensitivity improvements beyond these “Advanced” gravitational-wave detectors of the next generation, a rigorous quantum-mechanical description is certainly required [11].

In 2001, Kimble et al. [12] discussed quantum mechanical description of gravitational-wave detectors in detail and their paper has been regarded as a milestone paper of this topic and its ingredients are now regarded as the common knowledge in the community of the gravitational-wave detection. In their paper, the idea of the frequency dependent homodyne detection proposed by Vyatchanin, Matsko and Zubova [13] is explained as one of techniques to reduce

* E-mail address: kouji.nakamura@nao.ac.jp

† E-mail address: fujimoto.masa-katsu@nao.ac.jp

quantum noise and they claimed that “we can measure the output quadrature \hat{b}_θ defined by

$$\hat{b}_\theta := \cos \theta \hat{b}_1 + \sin \theta \hat{b}_2 \quad (1.1)$$

through the homodyne detection.” Here, \hat{b}_1 and \hat{b}_2 are the amplitude and phase quadrature in the two-photon formulation [14], which we briefly explain in Sec. III A in this paper, and θ is called the homodyne angle. Furthermore, as a result of their analysis of the interferometric gravitational-wave detectors, the output quadrature \hat{b}_θ includes gravitational-wave signal. Apart from the leakage of the classical carrier field to the output quadrature, we can formally write their output quadrature as

$$\hat{b}_\theta(\Omega) = R(\Omega, \theta) \left(\hat{h}_n(\Omega, \theta) + h(\Omega) \right), \quad (1.2)$$

where $h(\Omega)$ is a gravitational-wave signal in frequency domain, $\hat{h}_n(\Omega)$ is the noise operator which is given by the linear combination of the annihilation and creation operators of photons which inject to the main interferometer. The idea of the frequency dependent homodyne detection [12] is to choose the frequency dependent homodyne angle $\theta = \theta(\Omega)$ so that the output noise is minimized at the broad signal frequency range and their technique enables us to beat the sensitivity limit called “*standard quantum limit*” of gravitational-wave detectors which is also derived from Heisenberg’s uncertainty principle in quantum mechanics [15, 16].

In gravitational-wave detectors, a homodyne detection is one of the “readout scheme” which enables us to measure the photon field which includes gravitational-wave signals. There are three typical readout schemes in gravitational-wave detectors, which are called the heterodyne detection, DC readout scheme, and the homodyne detection. Heterodyne readout schemes were used in the early generations of the gravitational-wave detectors such as LIGO, Virgo, GEO600, and TAMA300. Since heterodyne readout schemes include some technical challenges, current generation of detectors use a DC readout scheme which directly measures the power of the output field. On the other hand, homodyne detections are not used in current gravitational-wave detectors, yet. However, homodyne detections are regarded as one of candidates of readout schemes for future gravitational-wave detectors, because these are expected to offers potential benefits over DC readout [17]. Therefore, homodyne detections are one of targets of the research and development activities for future gravitational-wave detectors.

In homodyne detections, we mix an additional photon coherent state to the output electric field from the main interferometer. The light source of this additional photon coherent state is called “local oscillator”. To produce appropriate homodyne angle $\theta = \theta(\Omega)$, the additional photon coherent state from the local oscillator must path a filter cavity before mixing with the output electric field from the main interferometer. Ref. [12] also includes a brief explanation of the properties of this filter cavity. However, in Ref. [12], there is no clear explanation of the issue how to accomplish the measurement of the operator \hat{b}_θ within quantum theory, though it is written that “the operator \hat{b}_θ is measured through the homodyne detection” with the citation of Refs. [13]. After this milestone paper [12], the same statement has been repeated in many papers [18] without any detailed explanation. In researches on gravitational-wave detectors, there is little literature which clearly explain the issue how to accomplish the measurement of operator \hat{b}_θ within quantum theory, yet, though there are some experimental papers on homodyne detections [19, 20].

In this paper, we examine the statement “the operator \hat{b}_θ is measured through the homodyne detection” through a view point of quantum theory. In quantum measurement theory, a homodyne detection is known as the measurement scheme of a linear combination of photon annihilation and creation operators [21]. In 1993, Wiseman and Milburn examined the homodyne detection in detail [22] motivated by the clarification of the property of the homodyne detection as a non-projection measurement in quantum theory. The arguments by Wiseman and Milburn were on the Schrödinger picture. In this paper, we re-examine the homodyne detection in the Heisenberg picture in quantum theory, which is more convenient to discuss some complicated interferometers than the Schrödinger picture.

Based on the understanding of the homodyne detection by Wiseman and Milburn, in this paper, we examine whether or not “the operator \hat{b}_θ can be measured through the homodyne detection.” We regard the meaning of the statement “the operator \hat{b}_θ can be measured” as “the expectation value of the operator \hat{b}_θ can be measured.” There are typically two types of the homodyne detections, which are called the “simple homodyne detection” and the “balanced homodyne detection,” respectively. In this paper, we examine whether or not “the expectation value of the operator \hat{b}_θ can be measured through the balanced homodyne detection.” In the homodyne detections, we inject an optical field to the beam splitter from the “local oscillator” as a reference field. This additional field is assumed to be in the coherent state with an appropriate complex amplitude $\gamma(\omega)$. In this paper, we assume that we already knew the complex amplitude of the coherent state from the local oscillator, i.e., not only the amplitude of $\gamma(\omega)$ but also its phase are completely known and controllable and we seek conditions for the complex amplitude $\gamma(\omega)$ of the coherent state to realize the measurement of the expectation value of the operator \hat{b}_θ . This standing point leads us the requirements for the complex amplitude to realize the statement “the expectation value of the operator \hat{b}_θ can be measured through the balanced homodyne detection.”

In a current quantum theoretical description of gravitational-wave detectors, the two-photon formulation developed by Caves and Schumaker is used [14]. In this formulation, we consider the quantum fluctuations at the frequency of the upper-sidebands $\omega_0 + \Omega$ and the lower-sidebands $\omega_0 - \Omega$ around the classical carrier field with the frequency ω_0 at linear level. The amplitude- and phase-quadratures in the two-photon formulation are given by the linear combination of these sideband-quadratures. When we consider the homodyne detection in two-photon formulation, we have the information of the results of the balanced homodyne detection with the upper- and lower-sidebands. For these reason, we regard that the general results from the balanced homodyne detection is given by a linear combination of these upper- and lower-sidebands. Therefore, in this paper, we examine whether or not “the expectation value of the operator \hat{b}_θ can be measured as the linear combination of the upper- and lower-sidebands from the output of the balanced homodyne detection.” However, as the result of this examination in Sec. III of this paper, we reach to the conclusion, “the expectation value of the operator \hat{b}_θ cannot be measured as the linear combination of the upper- and lower-sidebands from the output of the balanced homodyne detection.” This statement is the first assertion of this paper.

Keeping these our results of the examination in Sec. III in our mind, we consider the problem, “How to realize the measurement of the expectation value of the operator \hat{b}_θ in some way?” As the result of this consideration, we reach to the concept of the “*double balanced homodyne detection*”. The interferometer setup of our “double balanced homodyne detection” is completely same as the eight-port homodyne detection in literature [23–25]. The eight-port homodyne detection was originally proposed as a device to measure quasiprobability functions in quantum theory, and was used to discussed the phase measurement in quantum theory and the phase-corresponding self-adjoint operator. However, in this paper, we rediscovered the conceptually different use of the interferometer setup of the eight-port homodyne detection, which we call “double balanced homodyne detection.” Our double balanced homodyne detection was proposed in Ref. [26] as a measurement scheme to measure the expectation values of the photon annihilation and creation operators. In this paper, we show the statement, “the expectation value of the operator \hat{b}_θ can be measured through the double balanced homodyne detection.” This is the second assertion of this paper.

The organization of this paper is as follows. In Sec. II, we review the conventional homodyne detections from the view point of the Heisenberg picture. The ingredients of this section are based on Refs. [21, 22]. However, as we noted above, their description is in the Schrödinger picture and the aim of these references are different from ours. Our explanation of the homodyne detections in Sec. II is in the Heisenberg picture in quantum theory and is more compact than those in Refs. [21, 22]. In Sec. III, we consider the balanced homodyne detection in the two-photon formulation. We examine whether or not the statement, “the expectation value of the operator \hat{b}_θ can be measured as the linear combination of the upper- and lower-sidebands from the output of the balanced homodyne detection.” Then, we reach to the negative conclusion against this statement. We also summarize the possible cases which yields the linear combination of two quadratures among the amplitude quadrature \hat{b}_1 , the phase quadrature \hat{b}_2 , and their conjugate operators as the output of the balanced homodyne detection. In Sec. IV, we discussed the “double balanced homodyne detection” and show that the statement, “the expectation value of the operator \hat{b}_θ can be measured through the double balanced homodyne detection,” is correct. In Sec. V, we comment on the noise-spectral density in the case where we apply our “double balanced homodyne detection” to gravitational-wave detectors as their readout scheme. The final section (Sec. VI) is devoted to summary of this paper which includes the requirements for the coherent state from the local oscillator to realize our double balanced homodyne detection.

This paper is also regarded as the full paper version of Ref. [26] and includes ingredients of Ref. [26] with more detailed explanations.

II. CONVENTIONAL HOMODYNE DETECTIONS IN THE HEISENBERG PICTURE

In this section, we review quantum mechanical descriptions of the simple homodyne detection and the balanced homodyne detection [21, 22] in the Heisenberg picture. In Sec. II A, we describe the notation of the electric field in this paper. In Sec. II B, we describe the explanation of the simple homodyne detector. Then, in Sec. II C, we explain the balanced homodyne detection.

A. Electric field notation

As well known, the electric field operator at time t and the length of the propagation direction z in interferometers is described by

$$\hat{E}_a(t-z) = \hat{E}_a^{(+)}(t-z) + \hat{E}_a^{(-)}(t-z), \quad (2.1)$$

$$\hat{E}_a^{(-)}(t-z) = \left[\hat{E}_a^{(+)}(t-z) \right]^\dagger, \quad (2.2)$$

$$\hat{E}_a^{(+)}(t-z) = \int_0^\infty \sqrt{\frac{2\pi\hbar\omega}{\mathcal{A}c}} \hat{a}(\omega) e^{-i\omega(t-z)} \frac{d\omega}{2\pi}, \quad (2.3)$$

where $\hat{a}(\omega)$ is the photon annihilation operator associated with the electric field $\hat{E}_a(t-z)$ and \mathcal{A} is the cross-sectional area of the optical beam. The annihilation operator $\hat{a}(\omega)$ satisfies the usual commutation relation

$$[\hat{a}(\omega), \hat{a}^\dagger(\omega')] = 2\pi\delta(\omega - \omega'). \quad (2.4)$$

To discuss the input-output relation of the Michelson interferometer based on one-photon formulation, it is convenient to introduce operator $\hat{A}(\omega)$ defined by

$$\hat{A}(\omega) := \hat{a}(\omega)\Theta(\omega) + \hat{a}^\dagger(-\omega)\Theta(-\omega), \quad (2.5)$$

where $\Theta(\omega)$ is the Heaviside step function

$$\Theta(\omega) = \begin{cases} 1 & (\omega \geq 0), \\ 0 & (\omega < 0). \end{cases} \quad (2.6)$$

In terms of the operator $\hat{A}(\omega)$ defined by Eq. (2.5), the electric field $\hat{E}_a(t-z)$ in Eq. (2.1) is simply given by

$$\hat{E}_a(t) = \int_{-\infty}^{+\infty} \sqrt{\frac{2\pi\hbar|\omega|}{\mathcal{A}c}} \hat{A}(\omega) e^{-i\omega t} \frac{d\omega}{2\pi}. \quad (2.7)$$

Due to the property of the Dirac δ -function $\int_{-\infty}^{+\infty} dt e^{i(\omega' - \omega)t} = 2\pi\delta(\omega' - \omega)$, the inverse relation of Eq. (2.7) is given by

$$\hat{A}(\omega) = \sqrt{\frac{\mathcal{A}c}{2\pi\hbar|\omega|}} \int_{-\infty}^{+\infty} dt e^{i\omega t} \hat{E}_a(t). \quad (2.8)$$

Therefore, the operator $\hat{A}(\omega)$ includes complete information of the electric field operator $\hat{E}_a(t)$ and is convenient to derive the input-output relation of simple interferometers. Through this notation, we discuss the outputs of homodyne detections in the Heisenberg picture in quantum theory.

Throughout this paper, we denote the quadrature \hat{a} as that for the input field to the main interferometer. The state associated with this quadrature \hat{a} is usually the vacuum state. On the other hand, the output quadrature from the main interferometer is denoted by \hat{b} . Furthermore, in the homodyne detections, we inject the electric field whose state is a coherent state to the interferometer as a reference field. This coherent state comes from the *local oscillator*. The quadrature associated with the electric field from the local oscillator is denoted by \hat{l}_i . As noted above, the state associated with the quadrature \hat{l}_i is the coherent state $|\gamma\rangle_{l_i}$ which satisfies

$$\hat{l}_i(\omega)|\gamma\rangle_{l_i} = \gamma(\omega)|\gamma\rangle_{l_i}. \quad (2.9)$$

Here, $\gamma(\omega)$ is the complex eigenvalue for the coherent state. As well-known, the coherent state $|\gamma\rangle_{l_i}$ is given by the operation of the operator $D[\gamma]$ to the vacuum state $|0\rangle_{l_i}$ as

$$|\gamma\rangle_{l_i} = D[\gamma]|0\rangle_{l_i} := \exp \left[\int \frac{d\omega}{2\pi} \left(\gamma(\omega) \hat{l}_i^\dagger(\omega) - \gamma(\omega)^* \hat{l}_i(\omega) \right) \right] |0\rangle_{l_i}. \quad (2.10)$$

In this paper, we assume that the complex amplitude $\gamma(\omega)$ for the optical field from the local oscillator is completely controllable including its phase.

B. Simple homodyne detection

Here, we review the simple homodyne detection depicted in Fig. 1. In Fig. 1, the signal is in the electric field associated with the quadrature \hat{b} from the main interferometer. In this paper, we want to evaluate the signal in this electric field. The electric field from the local oscillator is the coherent state (2.10) with the complex amplitude $\gamma(\omega)$. The output signal field associated with the quadrature \hat{b} and the additional optical field from the local oscillator is mixed through the beam splitter with the transmissivity η . In the ideal case, this transmissivity is $\eta = 1/2$, but we dare to denote this transmissivity of the beam splitter for the homodyne detection by η . This is a simple model of the imperfection of the interferometer. In the simple homodyne detection, the photon number is detected by the photodetector (P.D.) at one of the port from the beam splitter as in Fig. 1.

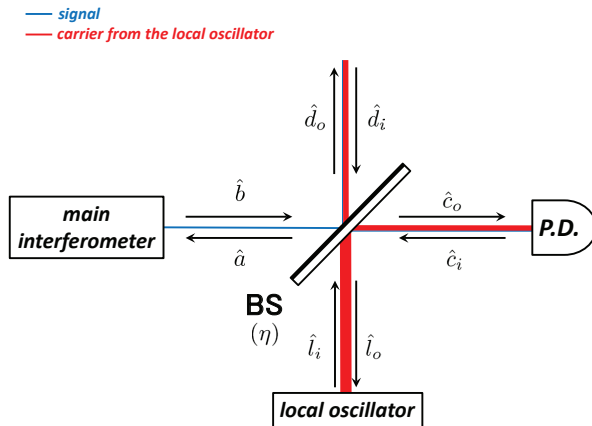


FIG. 1: Configuration of the interferometer for the simple homodyne detection. The notations of the quadratures \hat{a} , \hat{b} , \hat{c}_o , \hat{c}_i , \hat{d}_o , \hat{d}_i , \hat{l}_o , and \hat{l}_i are also given in this figure.

The output electric field \hat{E}_b from the main interferometer is denoted through the notation (2.7) as

$$\hat{E}_a(t) = \int_{-\infty}^{+\infty} \sqrt{\frac{2\pi\hbar|\omega|}{\mathcal{A}c}} \hat{B}(\omega) e^{-i\omega t} \frac{d\omega}{2\pi}, \quad (2.11)$$

where

$$\hat{B}(\omega) := \hat{b}(\omega)\Theta(\omega) + \hat{b}^\dagger(-\omega)\Theta(-\omega). \quad (2.12)$$

In the same notation, the electric field from the local oscillator is given by

$$\hat{E}_{l_i}(t) = \int_{-\infty}^{+\infty} \sqrt{\frac{2\pi\hbar|\omega|}{\mathcal{A}c}} \hat{L}_i(\omega) e^{-i\omega t} \frac{d\omega}{2\pi}, \quad (2.13)$$

where

$$\hat{L}_i(\omega) := \hat{l}_i(\omega)\Theta(\omega) + \hat{l}_i^\dagger(-\omega)\Theta(-\omega). \quad (2.14)$$

Furthermore, the electric field to be detected through the photodetector is given by

$$\hat{E}_{c_o}(t) = \int_{-\infty}^{+\infty} \sqrt{\frac{2\pi\hbar|\omega|}{\mathcal{A}c}} \hat{C}_o(\omega) e^{-i\omega t} \frac{d\omega}{2\pi}, \quad (2.15)$$

where

$$\hat{C}_o(\omega) := \hat{c}_o(\omega)\Theta(\omega) + \hat{c}_o^\dagger(-\omega)\Theta(-\omega). \quad (2.16)$$

At the beam splitter, the signal electric field $\hat{E}_b(t)$ and the electric field $\hat{E}_{l_i}(t)$ are mixed and the beam splitter output the electric field $\hat{E}_{c_o}(t)$ to the one of the ports. These fields are related by the relation

$$\hat{E}_{c_o}(t) = \sqrt{\eta}\hat{E}_b(t) + \sqrt{1-\eta}\hat{E}_{l_i}(t). \quad (2.17)$$

This relation given the quadrature relation as

$$\hat{c}_o(\omega) = \sqrt{\eta}\hat{b}(\omega) + \sqrt{1-\eta}\hat{l}_i(\omega). \quad (2.18)$$

Here, we assign the states for the independent electric field described in Fig. 1. As mentioned above, the electric field from the local oscillator is in the coherent state (2.10). In addition to this state, the electric fields associated with the quadratures \hat{d}_i and \hat{c}_i are injected into the beam splitter. In this paper, we regard that the electric fields associated with the quadratures \hat{d}_i and \hat{c}_i are in their vacua, respectively. The junction condition for the electric fields at the beam splitter is given by

$$\hat{E}_a(t) = \sqrt{\eta}\hat{E}_{c_i}(t) - \sqrt{1-\eta}\hat{E}_{d_i}(t). \quad (2.19)$$

In terms of the quadratures, this relation is given by

$$\hat{a}(\omega) = \sqrt{\eta}\hat{c}_i(\omega) - \sqrt{1-\eta}\hat{d}_i(\omega). \quad (2.20)$$

Due to this relation (2.20), the state associated with the quadrature \hat{a} is described by the vacuum states for the quadratures \hat{d}_i and \hat{c}_i .

Usually, the state associated with the quadrature \hat{b} depends on the state of the input field associated with the quadrature \hat{a} into the main interferometer and the other fields of optical fields which inject to the main interferometer [12, 18]. Furthermore, the electric field associated with the quadrature \hat{b} may include the information of classical forces as in the case of gravitational-wave detectors. In this paper, we regard that the electric field associated with the quadrature \hat{b} includes the signal of the classical forces and the information of this classical forces are measured through the expectation value of the quadrature \hat{b} . For this reason, we evaluate the expectation values for this electric field.

To evaluate the expectation value of the quadrature \hat{b} , we have to specify the state of the total system. Here, we assume that this state of the total system is given by

$$|\Psi\rangle = |\gamma\rangle_{l_i} \otimes |0\rangle_{c_i} \otimes |0\rangle_{d_i} \otimes |\psi\rangle_{main}, \quad (2.21)$$

where the state $|\psi\rangle_{main}$ is the state for the electric fields associated with the main interferometer, which is independent of the states $|\gamma\rangle_{l_i}$, $|0\rangle_{c_i}$, and $|0\rangle_{d_i}$, for example, the injected field from the optical light source. As noted above, the output quadrature \hat{b} may depends on the input quadrature \hat{a} and this input quadrature \hat{a} is related to the quadratures \hat{c}_i and \hat{d}_i through Eq. (2.20). Therefore, strictly speaking, the expectation value of the quadrature \hat{b} means that

$$\langle \hat{b} \rangle = \langle \psi |_{main} \otimes \langle 0 |_{d_i} \otimes \langle 0 |_{c_i} \hat{b} | 0 \rangle_{c_i} \otimes | 0 \rangle_{d_i} \otimes |\psi\rangle_{main}, \quad (2.22)$$

but we denote simply

$$\langle \hat{b} \rangle := \langle \Psi | \hat{b} | \Psi \rangle. \quad (2.23)$$

The photodetector (P.D.) in Fig. 1 detects the photon number of the electric field associated with the annihilation operator \hat{c}_o . So, we evaluate the expectation value of the photon number operator $\hat{n}_{c_o}(\omega) := \hat{c}_o^\dagger(\omega)\hat{c}_o(\omega)$. From the condition at the beam splitter, we obtain

$$\hat{n}_{c_o}(\omega) = \left(\sqrt{\eta}\hat{b}^\dagger(\omega) + \sqrt{1-\eta}\hat{l}_i^\dagger(\omega) \right) \left(\sqrt{\eta}\hat{b}(\omega) + \sqrt{1-\eta}\hat{l}_i(\omega) \right). \quad (2.24)$$

Through the definition of the coherent state (2.9), the expectation value for this number operator (2.24) under the state (2.21) for the total system is given by

$$\langle \hat{n}_{c_o}(\omega) \rangle := \langle \Psi | \hat{n}_{c_o}(\omega) | \Psi \rangle \quad (2.25)$$

$$= \eta \langle \hat{n}_b(\omega) \rangle + (1-\eta) |\gamma(\omega)|^2 + \sqrt{\eta(1-\eta)} \left\langle \gamma^*(\omega)\hat{b}(\omega) + \gamma(\omega)\hat{b}^\dagger(\omega) \right\rangle, \quad (2.26)$$

where we defined

$$\langle \hat{n}_b(\omega) \rangle = \langle \hat{b}^\dagger(\omega) \hat{b}(\omega) \rangle := \langle \Psi | \hat{b}^\dagger(\omega) \hat{b}(\omega) | \Psi \rangle, \quad (2.27)$$

$$\langle \gamma^*(\omega) \hat{b}(\omega) + \gamma(\omega) \hat{b}^\dagger(\omega) \rangle := \langle \Psi | \left(\gamma^*(\omega) \hat{b}(\omega) + \gamma(\omega) \hat{b}^\dagger(\omega) \right) | \Psi \rangle. \quad (2.28)$$

As we assumed above, $\gamma(\omega)$ is a known complex function of ω . Therefore, we can substitute the term

$$(1 - \eta) |\gamma(\omega)|^2 \quad (2.29)$$

from the expectation value $\langle \hat{n}_{c_o}(\omega) \rangle$, which is the dominant term in Eq. (2.26) if we consider the situation where the absolute value of $\gamma(\omega)$ is very large. In this situation, we can neglect the first term $\eta \langle \hat{n}_b(\omega) \rangle$ from the expectation value (2.26), since this term is smaller contribution than the last term in Eq. (2.26). Then, we can measure the expectation value of the linear combination

$$\gamma^*(\omega) \hat{b}(\omega) + \gamma(\omega) \hat{b}^\dagger(\omega) \quad (2.30)$$

of the annihilation- and creation operators for the output field as the subdominant contribution. This is the simple homodyne detection depicted in Fig. 1. We note that the large $\gamma(\omega)$ is essential in this simple homodyne detection. In this case, the first term $\eta \langle \hat{n}_b(\omega) \rangle$ in Eq. (2.26) is regarded as the small noise when we measure the expectation value of the combination (2.30).

C. Balanced homodyne detection

Next, we review the balanced homodyne detection which is depicted in Fig. 2. The optical configuration of the balanced homodyne detection is almost similar to the simple homodyne detection depicted in Fig. 1, but the difference is in the additional photon detection through the photodetector (D2 in Fig. 2) at the port of the beam splitter which is absent in the simple homodyne detection. In the balanced homodyne detection, we detect photons through the photodetectors D1 and D2 and measure the difference between them.

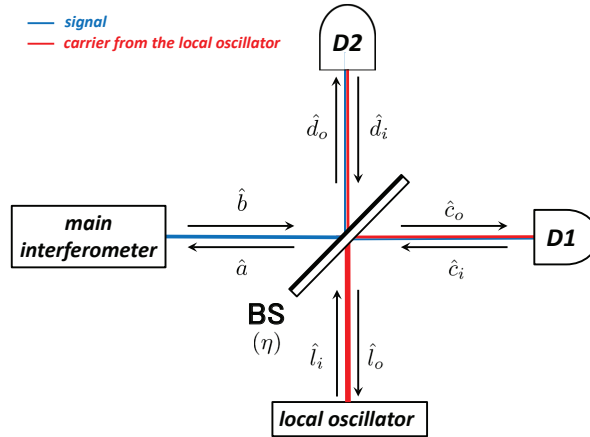


FIG. 2: Configuration of the interferometer for the balanced homodyne detection. This notation of the quadratures are same as those in Fig. 1.

To discuss the output of the balanced homodyne detection, we consider the photon number operators detected by the photodetectors D1 and D2 in Fig. 2, respectively. At the photodetector D1, we count the photon number which expressed the operator (2.24) in Sec. II B. Since the total state of the system is same as the state (2.21) in the case of the simple homodyne detector, the expectation value of the operator (2.24) is also given by Eq. (2.26) in Sec. II B.

In the balanced homodyne detection, we also detect the photon number through the photodetector D2. Following the notation of quadratures depicted in Fig. 2, the photon number operator which is detected at the photodetector D2 is given by $\hat{n}_{d_o}(\omega) := \hat{d}_o^\dagger(\omega) \hat{d}_o(\omega)$. The output electric field $\hat{E}_{d_o}(t)$ is produced through the mixing of the signal

electric field $\hat{E}_b(t)$ and the electric field $\hat{E}_{l_i}(t)$ from the local oscillator at the beam splitter. These fields are related by the relation

$$\hat{E}_{d_o}(t) = \sqrt{\eta}\hat{E}_b(t) - \sqrt{1-\eta}\hat{E}_{l_i}(t). \quad (2.31)$$

This relation given the quadrature relation as

$$\hat{d}_o(\omega) = \sqrt{\eta}\hat{b}(\omega) - \sqrt{1-\eta}\hat{l}_i(\omega). \quad (2.32)$$

Then, the photon number operator $\hat{n}_{d_o}(\omega)$ is given by

$$\hat{n}_{d_o}(\omega) = \left(\sqrt{\eta}\hat{l}_i(\omega) - \sqrt{1-\eta}\hat{b}(\omega)\right)^\dagger \left(\sqrt{\eta}\hat{l}_i(\omega) - \sqrt{1-\eta}\hat{b}(\omega)\right). \quad (2.33)$$

The expectation value of the operator $\hat{n}_{d_o}(\omega)$ in the state (2.21) is given by

$$\begin{aligned} \langle \hat{n}_{d_o}(\omega) \rangle &:= \langle \Psi | \hat{n}_{d_o}(\omega) | \Psi \rangle \\ &= (1-\eta)\langle \hat{n}_b(\omega) \rangle + \eta|\gamma(\omega)|^2 - \sqrt{\eta(1-\eta)} \left\langle \gamma^*(\omega)\hat{b}(\omega) + \gamma(\omega)\hat{b}^\dagger(\omega) \right\rangle, \end{aligned} \quad (2.34)$$

where we used Eqs. (2.27) and (2.28).

Through Eqs. (2.26) and (2.34), we can eliminate the term proportional to $\langle \hat{n}_b(\omega) \rangle$, which is regarded as the small noise term in the simple homodyne detection in Sec. II B. Actually, taking the linear combination of Eqs. (2.26) and (2.34), we obtain

$$\begin{aligned} &(1-\eta)\langle \hat{n}_{c_o}(\omega) \rangle - \eta\langle \hat{n}_{d_o}(\omega) \rangle \\ &= (1-2\eta)|\gamma(\omega)|^2 + \sqrt{\eta(1-\eta)} \left\langle \gamma^*(\omega)\hat{b}(\omega) + \gamma(\omega)\hat{b}^\dagger(\omega) \right\rangle. \end{aligned} \quad (2.35)$$

Since $\gamma(\omega)$ is a known complex function, we can always subtract the first term in Eq. (2.35) from the output signal. Then, we can unambiguously measure the linear combination of the quadrature $\hat{b}(\omega)$ and $\hat{b}^\dagger(\omega)$ as

$$\left\langle \gamma^*(\omega)\hat{b}(\omega) + \gamma(\omega)\hat{b}^\dagger(\omega) \right\rangle = \frac{(1-\eta)\langle \hat{n}_{c_o}(\omega) \rangle - \eta\langle \hat{n}_{d_o}(\omega) \rangle - (1-2\eta)|\gamma(\omega)|^2}{\sqrt{\eta(1-\eta)}}. \quad (2.36)$$

This is the balanced homodyne detection.

The right-hand side of Eq. (2.36) is also regarded as the expectation value of the operator $\hat{s}(\omega)$ defined by

$$\hat{s}(\omega) := \frac{1}{(\eta(1-\eta))^{1/2}} \left\{ (1-\eta)\hat{n}_{c_o}(\omega) - \eta\hat{n}_{d_o}(\omega) - (1-2\eta)|\gamma(\omega)|^2 \right\}, \quad (2.37)$$

$$= \hat{l}_i^\dagger(\omega)\hat{b}(\omega) + \hat{b}^\dagger(\omega)\hat{l}_i(\omega) + \frac{1-2\eta}{\sqrt{\eta(1-\eta)}} \left(\hat{l}_i^\dagger(\omega)\hat{l}_i(\omega) - |\gamma(\omega)|^2 \right), \quad (2.38)$$

where we used Eqs. (2.24) and (2.33). Actually, the expectation value of the operator (2.38) under the state (2.21) yields

$$\langle \hat{s}(\omega) \rangle = \left\langle \gamma^*(\omega)\hat{b}(\omega) + \hat{b}^\dagger(\omega)\gamma(\omega) \right\rangle. \quad (2.39)$$

Here, we note that the operator $\hat{s}(\omega)$ is a self-adjoint operator. This is due to the fact that the photon number operators are self-adjoint and $\hat{s}(\omega)$ is given by the linear combination of these number operators with real coefficients. Therefore, the expectation value $\langle \hat{s}(\omega) \rangle$ of the operator $\hat{s}(\omega)$ must be real. This can easily be seen from the expression of Eq. (2.39).

Before closing this section, we evaluate the covariance of the operator $\hat{s}(\omega)$ by

$$\text{Cov}[\hat{s}(\omega), \hat{s}(\omega')] := \langle \hat{s}(\omega)\hat{s}(\omega') \rangle - \langle \hat{s}(\omega) \rangle \langle \hat{s}(\omega') \rangle. \quad (2.40)$$

Through the expectation value (2.39), this covariance is given by

$$\begin{aligned} &\text{Cov}[\hat{s}(\omega), \hat{s}(\omega')] \\ &= \text{Cov} \left[\gamma^*(\omega)\hat{b}(\omega) + \gamma(\omega)\hat{b}^\dagger(\omega), \gamma^*(\omega')\hat{b}(\omega') + \gamma(\omega')\hat{b}^\dagger(\omega') \right] \\ &\quad + 2\pi\delta(\omega - \omega') \langle \hat{n}_b(\omega) \rangle \\ &\quad + 2\pi\delta(\omega - \omega') \frac{(1-2\eta)}{\sqrt{\eta(1-\eta)}} \left(\left\langle \gamma^*(\omega)\hat{b}(\omega) + \gamma(\omega)\hat{b}^\dagger(\omega) \right\rangle + \frac{(1-2\eta)|\gamma(\omega)|^2}{\sqrt{\eta(1-\eta)}} \right). \end{aligned} \quad (2.41)$$

We note that the second line in the right-hand side comes from the quantum fluctuations which characterized by the coherent state of the optical field from the local oscillator and the third line is due to the imperfection of the beam splitter.

III. BALANCED HOMODYNE DETECTION IN THE TWO-PHOTON FORMULATION

In this section, we consider the situation which is discussed in gravitational-wave detectors. In the community of gravitational-wave detections, the two-photon formulation [14] is used. In this formulation, we consider the sideband picture of fluctuations in the optical fields whose frequencies are given by $\omega_0 \pm \Omega$ around the classical carrier field with the frequency ω_0 . This concentration of the mode $\omega_0 \pm \Omega$ is based on the situation where there is the classical carrier field with the frequency ω_0 and we want to discuss the fluctuations at the frequency $\omega_0 \pm \Omega$ around this classical carrier. Almost all current arguments of the gravitational-wave detectors are based on this formulation. In the case of the gravitational-wave detectors, we concentrate only on the modes of fluctuations with the frequencies $\omega_0 \gg \Omega$. The two-photon formulation in Refs. [14] was formulated to treat this situation.

In Sec. III A, we introduce the amplitude quadrature \hat{b}_1 and phase-quadratures \hat{b}_2 , which are basic quadratures in discussions of quantum noises in gravitational-wave detectors. In Sec. III B, we examine whether or not we can measure the combination $\cos \theta \hat{b}_1 + \sin \theta \hat{b}_2$ through the simple application of the balanced homodyne detection reviewed in Sec. II C. Here, θ is called the ‘‘homodyne angle’’ in literature [12]. In many literature of the community of gravitational-wave detection, it has been written that the combination $\cos \theta \hat{b}_1 + \sin \theta \hat{b}_2$ can be detected through the homodyne detection [12, 13]. However, we show that we cannot measure this combination by the simple application of the balanced homodyne detection reviewed in Sec. II C. In Sec. III C, we describe the summary and remarks of the examination in Sec. III B.

A. Amplitude quadrature and phase quadrature

Keeping in our mind the above situation $\omega_0 \gg \Omega$ of the two-photon formulation, we introduce variables \hat{b}_\pm , \hat{l}_\pm , and γ_\pm as

$$\hat{b}_\pm(\Omega) := \hat{b}(\omega_0 \pm \Omega), \quad (3.1)$$

$$\hat{l}_{i\pm}(\Omega) := \hat{l}_i(\omega_0 \pm \Omega), \quad (3.2)$$

$$\gamma_\pm(\Omega) := \gamma(\omega_0 \pm \Omega). \quad (3.3)$$

In this situation, the operator (2.38) of the homodyne detection is given by

$$\hat{s}_\pm = \hat{l}_{i\pm}^\dagger \hat{b}_\pm + \hat{b}_\pm^\dagger \hat{l}_{i\pm} + \frac{1-2\eta}{\sqrt{\eta(1-\eta)}} \left(\hat{l}_{i\pm}^\dagger \hat{l}_{i\pm} - |\gamma_\pm|^2 \right). \quad (3.4)$$

Here, we omitted the notations of the explicit dependence on Ω in the expression (3.4), for simplicity.

Further, we introduce the amplitude and phase quadratures as

$$\hat{b}_1 := \frac{1}{\sqrt{2}} \left(\hat{b}_+ + \hat{b}_-^\dagger \right), \quad \hat{b}_2 := \frac{1}{\sqrt{2}i} \left(\hat{b}_+ - \hat{b}_-^\dagger \right). \quad (3.5)$$

Under the existence of the classical carrier field which proportional to $\cos \omega_0 t$, \bar{b}_1 and \hat{b}_2 are regarded as the quadratures for the amplitude fluctuations and the phase fluctuations, respectively. The definitions (3.5) are equivalent to

$$\hat{b}_+ := \frac{1}{\sqrt{2}} \left(\hat{b}_1 + i\hat{b}_2 \right), \quad \hat{b}_- := \frac{1}{\sqrt{2}} \left(\hat{b}_1^\dagger + i\hat{b}_2^\dagger \right) \quad (3.6)$$

and

$$\hat{b}_+^\dagger := \frac{1}{\sqrt{2}} \left(\hat{b}_1^\dagger - i\hat{b}_2^\dagger \right), \quad \hat{b}_-^\dagger := \frac{1}{\sqrt{2}} \left(\hat{b}_1 - i\hat{b}_2 \right). \quad (3.7)$$

As mentioned above, the aim of this section is to examine whether or not the direct measurement of the quadrature $\cos \theta \hat{b}_1 + \sin \theta \hat{b}_2$ with the homodyne angle θ is possible through the simple application of the balanced homodyne

detection described in Sec. II C. To carry out this examination, we have to consider the expectation values of the operator \hat{s}_\pm defined by Eq. (3.4) as

$$\langle \hat{s}_+ \rangle = \langle \gamma_+^* \hat{b}_+ + \hat{b}_+^\dagger \gamma_+ \rangle, \quad \langle \hat{s}_- \rangle = \langle \gamma_-^* \hat{b}_- + \hat{b}_-^\dagger \gamma_- \rangle. \quad (3.8)$$

Substituting Eqs. (3.6) and (3.7) into Eqs. (3.8) and taking linear combination of $\langle \hat{s}_+ \rangle$ and $\langle \hat{s}_- \rangle$, we obtain

$$\begin{aligned} \alpha \langle \hat{s}_+ \rangle + \beta \langle \hat{s}_- \rangle = \frac{1}{\sqrt{2}} \langle & (\alpha \gamma_+^* + \beta \gamma_-) \hat{b}_1 + i (\alpha \gamma_+^* - \beta \gamma_-) \hat{b}_2 \\ & + (\alpha \gamma_+ + \beta \gamma_-^*) \hat{b}_1^\dagger + i (-\alpha \gamma_+ + \beta \gamma_-^*) \hat{b}_2^\dagger \rangle. \end{aligned} \quad (3.9)$$

The linear combination (3.9) yields the possible output signal by choosing the parameter α and β which are completely controllable in the data taking procedure. Furthermore, we assume that the complex amplitudes γ_\pm of the coherent state from the local oscillator are also controllable in the experiment.

B. Can we measure the expectation value of \hat{b}_θ by the simple application of the balanced homodyne detection?

Here, we examine whether or not we can measure the linear combination $\hat{b}_\theta := \cos \theta \hat{b}_1 + \sin \theta \hat{b}_2$ through an appropriate choice of α , β , and γ_\pm . More generally, in this subsection, we consider the cases where the output signal (3.9) yields the linear combination of the two quadratures among \hat{b}_1 , \hat{b}_1^\dagger , \hat{b}_2 , and \hat{b}_2^\dagger . To do this, we treat following six cases, separately:

1. Linear combination of \hat{b}_1 and \hat{b}_2

Here, we check whether or not the linear combination (3.9) is expressed by a linear combination of \hat{b}_1 and \hat{b}_2 . This should be accomplished by the equation of the matrix form:

$$\begin{pmatrix} \gamma_+ & \gamma_-^* \\ -\gamma_+ & \gamma_-^* \end{pmatrix} \begin{pmatrix} \alpha \\ \beta \end{pmatrix} = \begin{pmatrix} 0 \\ 0 \end{pmatrix}. \quad (3.10)$$

If a nontrivial solution $(\alpha, \beta) \neq (0, 0)$ to Eq. (3.10) exists, the determinant of the matrix

$$\begin{pmatrix} \gamma_+ & \gamma_-^* \\ -\gamma_+ & \gamma_-^* \end{pmatrix} \quad (3.11)$$

should vanish, i.e., $2\gamma_+ \gamma_-^* = 0$. This implies that $\gamma_+ = 0$ or $\gamma_- = 0$. These cases are meaningless as balanced homodyne detections. This fact implies that the linear combination of $\langle \hat{s}_\pm \rangle$ does not give expectation values of the linear combination of \hat{b}_1 and \hat{b}_2 , by itself. This result directly means that the output signal (3.9) never yields $\hat{b}_\theta := \cos \theta \hat{b}_1 + \sin \theta \hat{b}_2$.

2. Linear combination of \hat{b}_1 and \hat{b}_1^\dagger

Here, we check whether or not Eq. (3.9) yields a linear combination of \hat{b}_1 and \hat{b}_1^\dagger . This situation should be accomplished by the equations of the matrix form:

$$\begin{pmatrix} \gamma_+^* & -\gamma_- \\ -\gamma_+ & \gamma_-^* \end{pmatrix} \begin{pmatrix} \alpha \\ \beta \end{pmatrix} = \begin{pmatrix} 0 \\ 0 \end{pmatrix}. \quad (3.12)$$

If a nontrivial solution $(\alpha, \beta) \neq (0, 0)$ to Eq. (3.12) exists, the determinant of the matrix

$$\begin{pmatrix} \gamma_+^* & -\gamma_- \\ -\gamma_+ & \gamma_-^* \end{pmatrix} \quad (3.13)$$

should vanish : $(\gamma_+\gamma_-)^* = \gamma_+\gamma_-$, i.e., $\gamma_+\gamma_-$ is real and we may choose so that

$$\gamma_+ = |\gamma_+|e^{i\theta}, \quad \gamma_- = |\gamma_-|e^{-i\theta}. \quad (3.14)$$

Substituting these expressions into Eqs. (3.12), we obtain

$$\beta = \frac{|\gamma_+|}{|\gamma_-|}\alpha. \quad (3.15)$$

Furthermore, substituting Eqs. (3.14) and (3.15) into Eq. (3.9), we obtain

$$\frac{\langle \hat{s}_+ \rangle}{|\gamma_+|} + \frac{\langle \hat{s}_- \rangle}{|\gamma_-|} = \sqrt{2} \langle \hat{b}_1 e^{-i\theta} + \hat{b}_1^\dagger e^{+i\theta} \rangle. \quad (3.16)$$

3. Linear combination of \hat{b}_1 and \hat{b}_2^\dagger

Here, we check whether or not Eq. (3.9) is expressed the linear combination of \hat{b}_1 and \hat{b}_2^\dagger . In this case, the following conditions should be satisfied:

$$\begin{pmatrix} \gamma_+^* & -\gamma_- \\ \gamma_+ & \gamma_-^* \end{pmatrix} \begin{pmatrix} \alpha \\ \beta \end{pmatrix} = \begin{pmatrix} 0 \\ 0 \end{pmatrix}. \quad (3.17)$$

The condition for the existence of the nontrivial solution $(\alpha, \beta) \neq (0, 0)$ to Eq. (3.17) is $(\gamma_+\gamma_-)^* = -\gamma_+\gamma_-$, i.e., $\gamma_+\gamma_-$ is purely imaginary. Therefore, we may choose γ_\pm as

$$\gamma_+ = |\gamma_+|e^{+i\theta}, \quad \gamma_- = i|\gamma_-|e^{-i\theta}. \quad (3.18)$$

Substituting Eq. (3.18) into Eq. (3.17), we obtain the relation

$$\beta = -i \frac{|\gamma_+|}{|\gamma_-|} \alpha \quad (3.19)$$

Furthermore, substituting Eqs. (3.18) and (3.19) into Eq. (3.9), we obtain

$$\frac{\langle \hat{s}_+ \rangle}{|\gamma_+|} - i \frac{\langle \hat{s}_- \rangle}{|\gamma_-|} = \sqrt{2} \langle e^{-i\theta} \hat{b}_1 - i e^{+i\theta} \hat{b}_2^\dagger \rangle. \quad (3.20)$$

4. Linear combination of \hat{b}_1^\dagger and \hat{b}_2

Here, we check whether or not Eq. (3.9) yields the linear combination of \hat{b}_1^\dagger and \hat{b}_2 . This should be accomplished by the equation of the matrix form:

$$\begin{pmatrix} \gamma_+^* & \gamma_- \\ -\gamma_+ & \gamma_-^* \end{pmatrix} \begin{pmatrix} \alpha \\ \beta \end{pmatrix} = \begin{pmatrix} 0 \\ 0 \end{pmatrix}. \quad (3.21)$$

The existence of the nontrivial solution $(\alpha, \beta) \neq (0, 0)$ to Eq. (3.21) is guaranteed by the vanishing condition of the determinant of the matrix

$$\begin{pmatrix} \gamma_+^* & \gamma_- \\ -\gamma_+ & \gamma_-^* \end{pmatrix}. \quad (3.22)$$

This condition is given by $(\gamma_+\gamma_-)^* = -\gamma_+\gamma_-$, i.e., $\gamma_+\gamma_-$ is purely imaginary and we may choose γ_\pm as

$$\gamma_+ = |\gamma_+|e^{+i\theta}, \quad \gamma_- = i|\gamma_-|e^{-i\theta}. \quad (3.23)$$

Substituting Eq. (3.23) into Eq. (3.21), we obtain

$$\beta = i \frac{|\gamma_+|}{|\gamma_-|} \alpha. \quad (3.24)$$

Further, through Eqs. (3.23) and (3.24), the linear combination (3.9) is given by

$$\frac{\langle \hat{s}_+ \rangle}{|\gamma_+|} + i \frac{\langle \hat{s}_- \rangle}{|\gamma_-|} = \sqrt{2} \langle i e^{-i\theta} \hat{b}_2 + e^{+i\theta} \hat{b}_1^\dagger \rangle. \quad (3.25)$$

5. *Linear combination of \hat{b}_1^\dagger and \hat{b}_2^\dagger*

Here, we examine whether or not the linear combination (3.9) is given by a linear combination of \hat{b}_1^\dagger and \hat{b}_2^\dagger . This case is accomplished by the equation of the matrix form

$$\begin{pmatrix} \gamma_+^* & \gamma_- \\ \gamma_+^* & -\gamma_- \end{pmatrix} \begin{pmatrix} \alpha \\ \beta \end{pmatrix} = \begin{pmatrix} 0 \\ 0 \end{pmatrix}. \quad (3.26)$$

The existence of the nontrivial solution $(\alpha, \beta) \neq (0, 0)$ to Eq. (3.26) is given by $\gamma_+^* \gamma_-$, which implies that $\gamma_+ = 0$ or $\gamma_- = 0$. These are meaningless as balanced homodyne detections as in the case in Sec. III B 1. This fact implies that the linear combination (3.9) does not give expectation values of the linear combination of \hat{b}_1^\dagger and \hat{b}_2^\dagger . This is consistent with the result in Sec. III B 1.

6. *Linear combination of \hat{b}_2 and \hat{b}_2^\dagger*

Finally, we check whether the linear combination (3.9) is expressed by a linear combination of \hat{b}_2 and \hat{b}_2^\dagger , or not. This case is accomplished by the equation of the matrix form

$$\begin{pmatrix} \gamma_+^* & \gamma_- \\ \gamma_+ & \gamma_-^* \end{pmatrix} \begin{pmatrix} \alpha \\ \beta \end{pmatrix} = \begin{pmatrix} 0 \\ 0 \end{pmatrix}. \quad (3.27)$$

The existence of nontrivial solutions $(\alpha, \beta) \neq (0, 0)$ to Eq. (3.27) is guaranteed by the vanishing determinant of the matrix

$$\begin{pmatrix} \gamma_+^* & \gamma_- \\ \gamma_+ & \gamma_-^* \end{pmatrix}. \quad (3.28)$$

This condition is given by $(\gamma_+ \gamma_-)^* = \gamma_- \gamma_+$, which means that $\gamma_+ \gamma_-$ is real. Therefore, we may choose γ_\pm so that

$$\gamma_+ = |\gamma_+| e^{+i\theta}, \quad \gamma_- = |\gamma_-| e^{-i\theta}. \quad (3.29)$$

Through Eqs. (3.29) and (3.27), we obtain

$$\beta = -\alpha \frac{|\gamma_+|}{|\gamma_-|}. \quad (3.30)$$

Substituting Eqs. (3.29) and (3.30) into Eq. (3.9), we obtain

$$\frac{\langle \hat{s}_+ \rangle}{|\gamma_+|} - \frac{\langle \hat{s}_- \rangle}{|\gamma_-|} = \sqrt{2}i \langle e^{-i\theta} \hat{b}_2 - e^{+i\theta} \hat{b}_2^\dagger \rangle. \quad (3.31)$$

C. Remarks

We have seen that we cannot directly measure the linear combination of \hat{b}_1 and \hat{b}_2 in Sec. III B 1. Similarly, we cannot directly measure the linear combination of \hat{b}_1^\dagger and \hat{b}_2^\dagger as we have seen in Sec. III B 5. These two cases are consistent with each other. These also indicate that we cannot directly measure \hat{b}_θ through the simple application of the balanced homodyne detection reviewed in Sec. II C, though it is described in many literature [12, 13, 18] that the linear combination $\cos \theta \hat{b}_1 + \sin \theta \hat{b}_2$ can be measured through a homodyne detection.

On the other hand, as seen in Sec. III B 2, we can directly measure the linear combination of \hat{b}_1 and \hat{b}_1^\dagger through the linear combination of the expectation values $\langle \hat{s}_\pm \rangle$ with real coefficients α and β as seen in Eqs. (3.15) and (3.16). Namely, the addition of the expectation values $\langle \hat{s}_\pm \rangle$ normalized by $|\gamma_\pm|$, respectively, yields the linear combination of \hat{b}_1 and \hat{b}_1^\dagger with the coefficients which depends on the phase of the complex amplitude for the coherent state from the local oscillator. To accomplish this, the phase of the complex amplitude γ_\pm for the coherent state from the local oscillator should be opposite as seen in Eq. (3.14). This is an important requirement for the coherent state from the local oscillator.

Similarly, as seen in Sec. III B 6, we can also directly measure the linear combination of \hat{b}_2 and \hat{b}_2^\dagger through the linear combination of the expectation values $\langle \hat{s}_\pm \rangle$ with real coefficients α and β as seen in Eqs. (3.30) and (3.16). Namely,

Combination	Possible?	γ_+	γ_-	α - β relation
\hat{b}_1 and \hat{b}_2	×	—	—	—
\hat{b}_1 and \hat{b}_1^\dagger	○	$ \gamma_+ e^{+i\theta}$	$ \gamma_- e^{-i\theta}$	$\beta = \frac{ \gamma_+ }{ \gamma_- }\alpha$
\hat{b}_1 and \hat{b}_2^\dagger	○	$ \gamma_+ e^{+i\theta}$	$i \gamma_- e^{-i\theta}$	$\beta = -i\frac{ \gamma_+ }{ \gamma_- }\alpha$
\hat{b}_1^\dagger and \hat{b}_2	○	$ \gamma_+ e^{+i\theta}$	$i \gamma_- e^{-i\theta}$	$\beta = +i\frac{ \gamma_+ }{ \gamma_- }\alpha$
\hat{b}_1^\dagger and \hat{b}_2^\dagger	×	—	—	—
\hat{b}_2 and \hat{b}_2^\dagger	○	$ \gamma_+ e^{+i\theta}$	$ \gamma_- e^{-i\theta}$	$\beta = -\frac{ \gamma_+ }{ \gamma_- }\alpha$

TABLE I: Summary of the problem whether or not the linear combination (3.9) can be reduced to the linear combination of two quadratures. In this table, the value of γ_+ is always arbitrary except for the non-vanishing condition $\gamma_+ \neq 0$ but the corresponding choice of γ_- is nontrivial. This table indicates that the relative phase of γ_\pm is important for the reduction of Eq. (3.9) to the linear combination of two quadratures.

if we take the difference of $\langle \hat{s}_\pm \rangle$ normalized by $|\gamma_\pm|$, respectively, we obtain the linear combination of \hat{b}_2 and \hat{b}_2^\dagger with the coefficients which depends on the phase of the complex amplitude for the coherent state from the local oscillator. To accomplish this, the phase of the complex amplitude γ_\pm for the coherent state from the local oscillator should be opposite as seen in Eq. (3.29). As in the case of Sec. III B 2, the phase condition for the local oscillator also is crucial.

The results of the above arguments in Sec. III B is summarized in Table I. In addition to the choice of the relation of the coefficients α and β , Table I indicates that the relative phase of γ_\pm of the local oscillator is important for the reduction of the linear combination (3.9) to the linear combination of two quadratures from \hat{b}_1 , \hat{b}_2 , \hat{b}_1^\dagger , and \hat{b}_2^\dagger .

Two cases in Sec. III B 2 and Sec. III B 6 are the case of the real coefficients α and β . Since the operators \hat{s}_\pm are self-adjoint operators, the resulting operators are also self-adjoint. Interestingly, the complex coefficients α β of the linear combination of $\langle \hat{s}_\pm \rangle$ is also possible as seen in Sec. III B 3 and in Sec. III B 4. In these cases, the results are no longer self-adjoint operators in spite that the operators \hat{s}_\pm are self-adjoint. Therefore, we can calculate an expectation value of non-self-adjoint operators from the expectation values of the self-adjoint operators which can be directly calculable from the expectation values of photon number operators in the balanced homodyne detection reviewed in Sec. II C.

Finally, we also note that in any possible cases in Sec. III B, the phase control of the upper- and lower-sidebands is necessary. Namely, from the local oscillator, we have to introduce the coherent state with the complex amplitudes $\gamma_\pm = \gamma(\omega_0 \pm \Omega)$ for upper- and lower-sideband have the opposite phase as in Eqs. (3.14), (3.18), (3.23), and (3.29). Before these important requirements for the phase of γ_\pm , γ_\pm must have their non-vanishing support at the frequency $\omega_0 \pm \Omega$. These requirements for the coherent state from the local oscillator are also important results from our examination in this section.

IV. DOUBLE BALANCED HOMODYNE DETECTION

Through the understanding of the balanced homodyne detections based on the examinations in Sec. III, we propose the “double balanced homodyne detection” which enable us to measure the expectation values for the photon annihilation and creation operators themselves. Our assertion in our previous letter [26] comes from this consideration.

In Sec. IV A, we describe our theoretical proposal of a double balanced homodyne detection. In Sec. IV B, we propose a realization of our double balanced homodyne detection through the interferometer setup. In Sec. IV C, we discuss the field-dependence of the input field to the main interferometer and commutation relations of the quadratures in our proposal. In Sec. IV D, we show the double balanced homodyne detection through our interferometer setup enable us to measure the expectation values of the annihilation and creation operators for the output quadrature from the main interferometer. The ingredients of Sec. IV D includes that of our previous letter [26] with additional explanation in detail. Finally, in Sec. IV E, we show that the expectation value of the linear combination $\hat{b}_\theta := \cos\theta\hat{b}_1 + \sin\theta\hat{b}_2$ of

the output quadrature from the main interferometer can be measured through our interferometer setup.

In this section, we assume that the absolute value of the complex amplitudes γ_{\pm} for the upper- and lower-sidebands in the coherent state from the local oscillator are equal with each other, i.e., $|\gamma_{\pm}| =: |\gamma|$, for simplicity. Since we assumed that the complex amplitude for the coherent state from the local oscillator is completely controllable, this assumption is consistent with the premise of our analysis. Of course, the generalization to the case where $|\gamma_+| \neq |\gamma_-|$ is always possible and straightforward. Some parts of this generalization can be seen in Appendix A.

A. Theoretical proposal

In this subsection, we describe our theoretical proposal of the double balanced homodyne detection. In Sec. IV A 1, we describe how to realize the expectation values of \hat{b}_1 , \hat{b}_1^\dagger , \hat{b}_2 , or \hat{b}_2^\dagger in the calculations on papers. The idea in Sec. IV A 1 is extended in Sec. IV A 2 to the measurement of the linear combination $\cos\theta\hat{b}_1 + \sin\theta\hat{b}_2$.

1. Expectation values of \hat{b}_1 , \hat{b}_1^\dagger , \hat{b}_2 , and \hat{b}_2^\dagger

Here again, we consider the case in Sec. III B 2. In this case, the linear combination (3.9) is given by

$$\frac{1}{\sqrt{2}|\gamma|} (\langle \hat{s}_+ \rangle + \langle \hat{s}_- \rangle) = \langle \hat{b}_1 \rangle e^{-i\theta} + \langle \hat{b}_1^\dagger \rangle e^{+i\theta}, \quad (4.1)$$

where we assumed $|\gamma_{\pm}| = |\gamma|$. Since the complex amplitude γ including its phase is completely controllable, we may choose $\theta = 0$ or $\theta = \pi/2$, for example. In the case where $\theta = 0$, Eq. (4.1) is given by

$$\frac{1}{\sqrt{2}|\gamma|} (\langle \hat{s}_+ \rangle + \langle \hat{s}_- \rangle) \Big|_{\theta=0} = \langle \hat{b}_1 \rangle + \langle \hat{b}_1^\dagger \rangle. \quad (4.2)$$

On the other hand, when we choose $\theta = \pi/2$, Eq. (4.1) is given by

$$\frac{1}{\sqrt{2}|\gamma|} (\langle \hat{s}_+ \rangle + \langle \hat{s}_- \rangle) \Big|_{\theta=\pi/2} = -i\langle \hat{b}_1 \rangle + i\langle \hat{b}_1^\dagger \rangle. \quad (4.3)$$

If we can produce the results Eqs. (4.2) and (4.3) at the same time, we can calculate

$$\frac{1}{2\sqrt{2}|\gamma|} \left\{ (\langle \hat{s}_+ \rangle + \langle \hat{s}_- \rangle) \Big|_{\theta=0} + i(\langle \hat{s}_+ \rangle + \langle \hat{s}_- \rangle) \Big|_{\theta=\pi/2} \right\} = \langle \hat{b}_1 \rangle, \quad (4.4)$$

$$\frac{1}{2\sqrt{2}|\gamma|} \left\{ (\langle \hat{s}_+ \rangle + \langle \hat{s}_- \rangle) \Big|_{\theta=0} - i(\langle \hat{s}_+ \rangle + \langle \hat{s}_- \rangle) \Big|_{\theta=\pi/2} \right\} = \langle \hat{b}_1^\dagger \rangle. \quad (4.5)$$

Note that $\langle \hat{s}_{\pm} \rangle$ are measured from the photon number distribution in the frequency domain through the balanced homodyne detection. We also note that γ (i.e., γ_{\pm}) is controllable complex amplitude of the coherent state of photon from the local oscillator. Therefore, Eq. (4.4) and (4.5) imply that the expectation values $\langle \hat{b}_1 \rangle$ and $\langle \hat{b}_1^\dagger \rangle$ of the quadrature can be directly measured from these measurement, respectively, though the operators \hat{b}_1 is not self-adjoint operator. This situation is similar to the cases in Sec. III B 3 and Sec. III B 4.

Similar analysis is possible even in the case in Sec. III B 6. The results yield that we can calculate the expectation values of the quadrature $\langle \hat{b}_2 \rangle$ and $\langle \hat{b}_2^\dagger \rangle$ from the expectation values $\langle \hat{s}_{\pm} \rangle$ which can be calculated from the expectation values of photon number operators in the balanced homodyne detection. Actually, the result (3.31) in Sec. III B 6 is given by

$$\frac{1}{\sqrt{2}i|\gamma|} (\langle \hat{s}_+ \rangle - \langle \hat{s}_- \rangle) = e^{-i\theta} \langle \hat{b}_2 \rangle - e^{+i\theta} \langle \hat{b}_2^\dagger \rangle. \quad (4.6)$$

As in the case of Eq. (4.1), we obtain the expectation values $\langle \hat{b}_2 \rangle$ and $\langle \hat{b}_2^\dagger \rangle$ as follows:

$$\frac{1}{2\sqrt{2}|\gamma|} \left\{ -i(\langle \hat{s}_+ \rangle - \langle \hat{s}_- \rangle) \Big|_{\theta=0} + (\langle \hat{s}_+ \rangle - \langle \hat{s}_- \rangle) \Big|_{\theta=\pi/2} \right\} = \langle \hat{b}_2 \rangle, \quad (4.7)$$

$$\frac{1}{2\sqrt{2}|\gamma|} \left\{ i(\langle \hat{s}_+ \rangle - \langle \hat{s}_- \rangle) \Big|_{\theta=0} + (\langle \hat{s}_+ \rangle - \langle \hat{s}_- \rangle) \Big|_{\theta=\pi/2} \right\} = \langle \hat{b}_2^\dagger \rangle. \quad (4.8)$$

We note that Eq. (4.8) is important in the gravitational-wave detection, because the phase quadrature \hat{b}_2 includes gravitational wave signal in conventional interferometer.

2. Expectation value of $\cos \theta \hat{b}_1 + \sin \theta \hat{b}_2$

Inspecting analyses in Appendix A, we introduce from the operators \hat{t}_\pm which are defined by

$$\hat{t}_+ := \frac{1}{\sqrt{2}|\gamma|} (\hat{s}_+ + \hat{s}_-), \quad \hat{t}_- := \frac{1}{\sqrt{2}i|\gamma|} (\hat{s}_+ - \hat{s}_-) \quad (4.9)$$

to consider the expectation value of the operator $\cos \theta \hat{b}_1 + \sin \theta \hat{b}_2$. The reason for why we treat these operators is explained in Appendix A. Of course, we require $\theta_\pm = \theta$ as the requirement for the phase of the complex amplitudes γ_\pm as discussed in Appendix A. In addition, we assumed $|\gamma_\pm| = |\gamma|$ for simplicity.

From the expressions (3.4) of the operators \hat{s}_\pm , we obtain

$$\frac{\hat{s}_\pm}{|\gamma|} = \frac{\hat{l}_{i\pm}^\dagger}{|\gamma|} \hat{b}_\pm + \frac{\hat{l}_{i\pm}}{|\gamma|} \hat{b}_\pm^\dagger + \frac{1-2\eta}{\eta^{1/2}(1-\eta)^{1/2}} |\gamma| \left(\frac{\hat{l}_{i\pm}^\dagger}{|\gamma|} \frac{\hat{l}_{i\pm}}{|\gamma|} - 1 \right) \quad (4.10)$$

and the above operators \hat{t}_\pm are given by

$$\begin{aligned} \hat{t}_+ = \frac{1}{\sqrt{2}} \left\{ \frac{\hat{l}_{i+}^\dagger}{|\gamma|} \hat{b}_+ + \frac{\hat{l}_{i+}}{|\gamma|} \hat{b}_+^\dagger + \frac{1-2\eta}{\eta^{1/2}(1-\eta)^{1/2}} |\gamma| \left(\frac{\hat{l}_{i+}^\dagger}{|\gamma|} \frac{\hat{l}_{i+}}{|\gamma|} - 1 \right) \right. \\ \left. + \frac{\hat{l}_{i-}^\dagger}{|\gamma|} \hat{b}_- + \frac{\hat{l}_{i-}}{|\gamma|} \hat{b}_-^\dagger + \frac{1-2\eta}{\eta^{1/2}(1-\eta)^{1/2}} |\gamma| \left(\frac{\hat{l}_{i-}^\dagger}{|\gamma|} \frac{\hat{l}_{i-}}{|\gamma|} - 1 \right) \right\}, \end{aligned} \quad (4.11)$$

and

$$\begin{aligned} \hat{t}_- = \frac{1}{\sqrt{2}i} \left\{ \frac{\hat{l}_{i+}^\dagger}{|\gamma|} \hat{b}_+ + \frac{\hat{l}_{i+}}{|\gamma|} \hat{b}_+^\dagger + \frac{1-2\eta}{\eta^{1/2}(1-\eta)^{1/2}} |\gamma| \left(\frac{\hat{l}_{i+}^\dagger}{|\gamma|} \frac{\hat{l}_{i+}}{|\gamma|} - 1 \right) \right. \\ \left. - \frac{\hat{l}_{i-}^\dagger}{|\gamma|} \hat{b}_- - \frac{\hat{l}_{i-}}{|\gamma|} \hat{b}_-^\dagger - \frac{1-2\eta}{\eta^{1/2}(1-\eta)^{1/2}} |\gamma| \left(\frac{\hat{l}_{i-}^\dagger}{|\gamma|} \frac{\hat{l}_{i-}}{|\gamma|} - 1 \right) \right\}. \end{aligned} \quad (4.12)$$

The expectation value of the operators (4.11) and (4.12) with the requirement $\theta_\pm = \theta$ are given by

$$\langle \hat{t}_+ \rangle_{|\theta_\pm=\theta} = \frac{1}{\sqrt{2}} \langle e^{-i\theta} \hat{b}_+ + e^{+i\theta} \hat{b}_+^\dagger + e^{-i\theta} \hat{b}_- + e^{+i\theta} \hat{b}_-^\dagger \rangle \quad (4.13)$$

$$= \left\langle \left(\cos \theta \hat{b}_1 + \sin \theta \hat{b}_2 \right) + \left(\cos \theta \hat{b}_1 + \sin \theta \hat{b}_2 \right)^\dagger \right\rangle, \quad (4.14)$$

and

$$\langle \hat{t}_- \rangle_{|\theta_\pm=\theta} = \frac{1}{\sqrt{2}i} \langle e^{-i\theta} \hat{b}_+ + e^{+i\theta} \hat{b}_+^\dagger - e^{-i\theta} \hat{b}_- - e^{+i\theta} \hat{b}_-^\dagger \rangle \quad (4.15)$$

$$= \left\langle \left(-\sin \theta \hat{b}_1 + \cos \theta \hat{b}_2 \right) - \left(-\sin \theta \hat{b}_1 + \cos \theta \hat{b}_2 \right)^\dagger \right\rangle. \quad (4.16)$$

Here, we used the fact that the state for the quadratures \hat{l}_\pm is in the coherent state $|\gamma\rangle_{l_\pm}$ which is defined by (2.10) and

$$\hat{l}_\pm |\gamma\rangle_{l_i} = \gamma_\pm |\gamma\rangle_{l_\pm} = |\gamma| e^{+i\theta} |\gamma\rangle_{l_\pm} \quad (4.17)$$

and Eqs. (3.6). We note that Eq. (4.16) indicates that

$$\langle \hat{t}_- \rangle_{|\theta_\pm=\theta+\pi/2} = \left\langle \left(\cos \theta \hat{b}_1 + \sin \theta \hat{b}_2 \right) - \left(\cos \theta \hat{b}_1 + \sin \theta \hat{b}_2 \right)^\dagger \right\rangle. \quad (4.18)$$

From (4.14) and (4.18), we have obtained

$$\frac{1}{2} \left\{ \langle \hat{t}_+ \rangle_{|\theta_\pm=\theta} + \langle \hat{t}_- \rangle_{|\theta_\pm=\theta+\pi/2} \right\} = \left\langle \cos \theta \hat{b}_1 + \sin \theta \hat{b}_2 \right\rangle. \quad (4.19)$$

The expectation value of the operator \hat{s}_\pm are directly measured by the photon numbers through balanced homodyne detections. The complex amplitudes γ_\pm are completely controllable including their phases. Therefore, the expectation value

$$\frac{1}{2} \left\{ \langle \hat{t}_+ \rangle |_{\theta_\pm=\theta} + \langle \hat{t}_- \rangle |_{\theta_\pm=\theta+\pi/2} \right\} \quad (4.20)$$

is also calculable if the first term and the second term can be independently measured at the same time. This implies that the expectation value of the quadrature

$$\langle \cos \theta \hat{b}_1 + \sin \theta \hat{b}_2 \rangle \quad (4.21)$$

is also calculable from measurable quantities under the same situation. This is the desired result for the descriptions of the conventional homodyne detection in many literature of gravitational-wave detections, though this is the result of our double balance homodyne detection proposed here.

In the next section, we discuss how to realize this theoretical proposal through an interferometer setup.

B. A realization of our double balanced homodyne detection

In this subsection, we consider the realization of the measurement of the expectation value $\langle \cos \theta \hat{b}_1 + \sin \theta \hat{b}_2 \rangle$ through an interferometer setup. Our proposal of the interferometer configuration to realize this measurement is depicted in Fig. 3. This interferometer setup is so called the “eight-port homodyne detection” [23–25]. We call our use of the eight-port homodyne detection as “double balanced homodyne detection.” In Sec. IV B 1, we describe the outline of the interferometer setup for our double balanced homodyne detection in Fig. 3. In Sec. IV B 2, we explain about the separation of the signal field from the main interferometer through the beam splitter BS1. In Sec. IV B 3, we explain about the separation of the coherent state from the local oscillator through the beam splitter BS3. In Sec. IV B 4, we explain about the balanced homodyne detection through the beam splitter BS2. Finally, in Sec. IV B 5, we explain about the balanced homodyne detection through the beam splitter BS4. The results derived in this subsection lead to our main results in this paper.

1. Outline of double balanced homodyne detection

Here, we describe the outline of our proposal of the double balanced homodyne detection.

To measure the photon described by the operators (4.14) and (4.18) at the same time, we introduce two balanced homodyne detections. To carry out these two balanced homodyne detection, we separate the signal photon field associated with the quadrature \hat{b} from the main interferometer through the beam splitter BS1. Furthermore, we also separate the photon field associated with the quadrature \hat{l}_i from the local oscillator through the beam splitters BS3. One of the these separated set of the signal field associated with the quadrature $\hat{b}_{(1)}$ and the field associated with the quadrature $\hat{l}_{(0)}$ from the local oscillator are mixed at the beam splitter BS2 and this mixed fields are detected photodetectors D1 and D2 to carry out the usual balanced homodyne detection. In another set of these separated operator, the field from the local oscillator associated with the quadrature $\hat{l}_{(1)i}$ goes through the phase rotator PR and gain the additional $\pi/2$ -phase. We denote the quadrature for this phase-added field by $\hat{l}_{(1/4)i}$. This field and the separated signal field associated with the quadrature $\hat{b}_{(2)}$ are mixed the beam splitter BS4 and then detected by the photodetectors D3 and D4 to carry out the usual balanced homodyne detection.

2. Separation of the signal field

Now we analyze the photon field along the interferometer setup depicted in Fig. 3, in detail. First, at the 50:50 beam splitter 1 (BS1), the output signal \hat{b} from the main interferometer is separated into two parts, which we denote $\hat{b}_{(1)}$ and $\hat{b}_{(2)}$, respectively. In addition to the output quadrature \hat{b} , the additional noise source is inserted, which is denoted \hat{e}_i in Fig. 3. Then, at BS1, the quadratures \hat{b} , $\hat{b}_{(1)}$, $\hat{b}_{(2)}$, and \hat{e}_i are related as

$$\hat{b}_{(1)} = \frac{1}{\sqrt{2}} (\hat{b} - \hat{e}_i), \quad \hat{b}_{(2)} = \frac{1}{\sqrt{2}} (\hat{b} + \hat{e}_i) \quad (4.22)$$

through the field junction conditions at the BS1. We assume the state associated with the quadrature \hat{e}_i is vacuum.

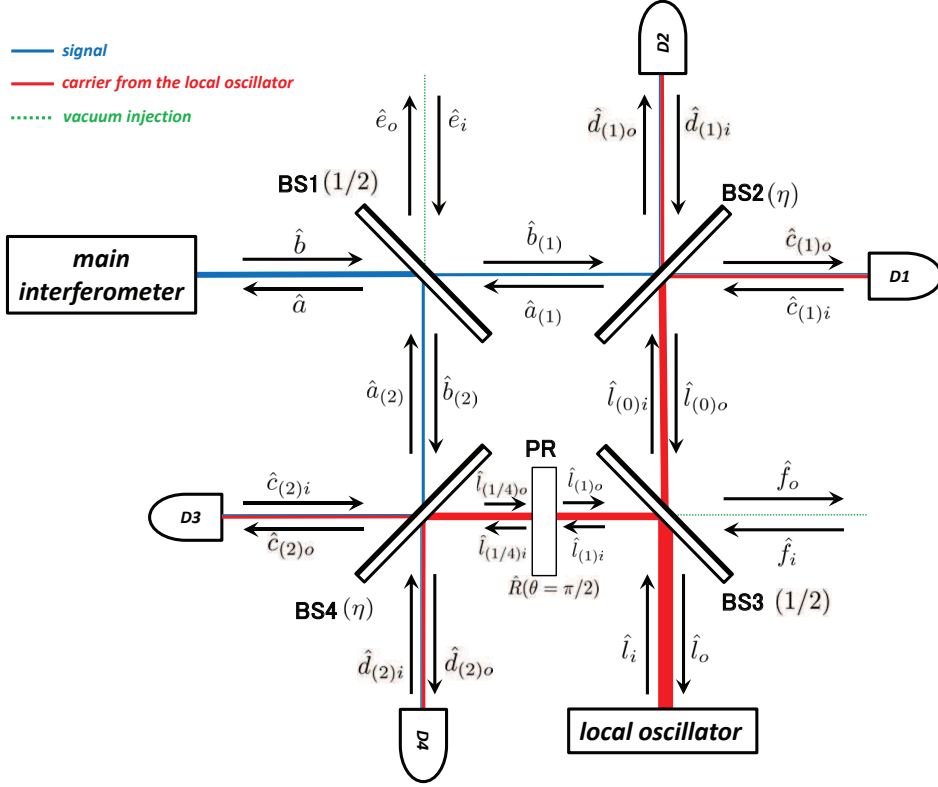


FIG. 3: A realization of the measurement process of the quadrature $\langle \cos \theta \hat{b}_1 + \sin \theta \hat{b}_2 \rangle$. In this figure, “BS” is the beam splitter, “PR” is the phase rotator. To measure the photon described by the operators (4.14) and (4.18) at the same time, we introduce two balanced homodyne detection. To carry out these two balanced homodyne detections, we separate the signal photon field associated with the quadrature \hat{b} from the main interferometer and the photon field associated with the quadrature \hat{l}_i from the local oscillator through the beam splitters BS1 and BS3, respectively. One of these two paths is used for the usual balanced homodyne detection through the beam splitter BS2 and the photodetectors D1 and D2. Along the other path, we introduce the phase rotator PR to introduce $\pi/2$ -phase difference in the photon field from the local oscillator and detect by the usual balanced homodyne detection after this phase addition through the beam splitter BS4 and the photodetector D3 and D2. We describe the paths of the signal photon field and the field from the local oscillator. The notation of the quadratures for the photon fields are also described in this figure. We consider the case where the transmittance η for BS2 and BS4 is not 1/2 as a simple model of imperfection of the interferometer setup.

3. Separation of the field from the local oscillator

At the 50:50 beam splitter 3 (BS3), the incident electric field from the local oscillator is in the coherent state and its quadrature is denoted by \hat{l}_i . Further, from the configuration depicted in Fig. 3, another incident field to BS3, which we denote its quadrature by \hat{f}_i , should be taken into account. On the other hand, the beam splitter BS3 separate the electric field into two paths. The electric field along one of these two paths goes from BS3 to BS2. We denote the quadrature associated with this electric field by $\hat{l}_{(0)i}$. On the other hand, the electric field along another path from BS3 is towards to the beam splitter 4 (BS4). We denote the quadrature associated with this electric field by $\hat{l}_{(1)i}$. By the beam splitter condition, quadratures $\hat{l}_{(0)i}$ and $\hat{l}_{(1)i}$ are determined by the equation

$$\hat{l}_{(0)i} = \frac{1}{\sqrt{2}} (\hat{l}_i - \hat{f}_i), \quad \hat{l}_{(1)i} = \frac{1}{\sqrt{2}} (\hat{l}_i + \hat{f}_i). \quad (4.23)$$

We also assume that the state associated with the quadrature \hat{f}_i is also vacuum. The field associated with the quadrature $\hat{l}_{(0)i}$ is used the balanced homodyne detection through the beam splitter 2 (BS2).

To make $\pi/2$ -phase difference in the electric field from the local oscillator as discussed in Sec. IV A, we introduce the phase rotator (PR) between BS3 and BS4. As shown in Appendix A in Ref. [12], the phase rotator operates the

rotation operator $R(\theta)$ defined by

$$R(\theta) = \exp \left\{ -i\theta \int_0^{+\infty} \frac{d\Omega}{2\pi} \left(\hat{l}_{(1)i+}^\dagger \hat{l}_{(1)i+} + \hat{l}_{(1)i-}^\dagger \hat{l}_{(1)i-} \right) \right\}. \quad (4.24)$$

The properties of this operator $R(\theta)$ is also summarized in Appendix B. The phase rotator (PR) in Fig. 3 is defined as a device which operates to the quadrature $\hat{l}_{(1)i}$ and produce the quantum field associated with the quadrature $\hat{l}_{(1/4)i}$ as the output field as

$$\hat{l}_{(1/4)i} = i\hat{l}_{(1)i} \quad (4.25)$$

which is shown in Appendix B. This quadrature $\hat{l}_{(1/4)i}$ is used the balanced homodyne detection through BS4.

4. Balanced homodyne detection through BS2

Now, we consider the balanced homodyne detection through the beam splitter BS2. Here, as a simple model of the imperfections of the interferometer configurations, we assume that the transmittance of the beamsplitter BS2 is η . The important incident fields to the beam splitter BS2 are $\hat{b}_{(1)}$ and $\hat{l}_{(0)i}$ and the important outgoing fields from BS2 are $\hat{c}_{(1)o}$ and $\hat{d}_{(1)o}$. At the BS2, these fields are related as

$$\hat{c}_{(1)o} = \sqrt{\eta}\hat{b}_{(1)} + \sqrt{1-\eta}\hat{l}_{(0)i}, \quad \hat{d}_{(1)o} = \sqrt{\eta}\hat{l}_{(0)i} - \sqrt{1-\eta}\hat{b}_{(1)}. \quad (4.26)$$

In the idealized case, $\eta = 1/2$ [26] but, in this paper, we denote the transmittance of the beam splitter BS2 is η as a simple model of imperfections of the interferometer setup.

The quadrature $\hat{b}_{(1)}$ is related to the direct output quadrature \hat{b} through the first equation in Eqs. (4.22) and the quadrature $\hat{l}_{(0)i}$ is related to the quadrature \hat{l}_i of the incident field from the local oscillator through the first equation in Eqs. (4.23). Then, Eqs. (4.26) are given by

$$\hat{c}_{(1)o} = \frac{1}{\sqrt{2}} \left(\sqrt{\eta}\hat{b} + \sqrt{1-\eta}\hat{l}_i \right) - \frac{1}{\sqrt{2}} \left(\sqrt{\eta}\hat{e}_i + \sqrt{1-\eta}\hat{f}_i \right), \quad (4.27)$$

$$\hat{d}_{(1)o} = \frac{1}{\sqrt{2}} \left(\sqrt{\eta}\hat{l}_i - \sqrt{1-\eta}\hat{b} \right) + \frac{1}{\sqrt{2}} \left(\sqrt{1-\eta}\hat{e}_i - \sqrt{\eta}\hat{f}_i \right). \quad (4.28)$$

Here, we note that the second terms in Eqs. (4.27) and (4.28) are the contribution of the incident vacuum field due to the interferometer configuration depicted in Fig. 3, respectively.

The photon numbers of the output fields associated with the quadratures $\hat{c}_{(1)o}$ and $\hat{d}_{(1)o}$ are detected through the photodetector D1 and D2 in Fig. 3, respectively, These photon number operators are defined by

$$\hat{n}_{c_{(1)o}} := \hat{c}_{(1)o}^\dagger \hat{c}_{(1)o}, \quad \hat{n}_{d_{(1)o}} := \hat{d}_{(1)o}^\dagger \hat{d}_{(1)o}. \quad (4.29)$$

Through Eqs. (4.27) and (4.28), these operators are given by in terms of the quadratures \hat{b} , \hat{l}_i , \hat{e}_i and \hat{f}_i . The expectation value of the photon number operator $\hat{n}_{c_{(1)o}}$, which is detected by the photodetector D1, is given by

$$\langle \hat{n}_{c_{(1)o}} \rangle = \frac{\eta}{2} \langle \hat{n}_b \rangle + \frac{\sqrt{\eta(1-\eta)}}{2} \langle \gamma^* \hat{b} + \gamma \hat{b}^\dagger \rangle + \frac{(1-\eta)}{2} |\gamma|^2. \quad (4.30)$$

On the other hand, the expectation value of the photon number operator $\hat{n}_{d_{(1)o}}$, which is detected by the photodetector D2, is given by

$$\langle \hat{n}_{d_{(1)o}} \rangle = \frac{\eta}{2} |\gamma|^2 - \frac{\sqrt{\eta(1-\eta)}}{2} \langle \gamma^* \hat{b} + \gamma \hat{b}^\dagger \rangle + \frac{1-\eta}{2} \langle \hat{n}_b \rangle. \quad (4.31)$$

In the derivation of Eqs. (4.30) and (4.31), we used the field associated with the quadrature \hat{l}_i is in the coherent state with the complex amplitude γ and the fields associated with the quadratures \hat{e}_i and \hat{f}_i are in vacua, respectively. As in the case of the conventional balanced homodyne detection in Sec. II C, we obtain

$$\frac{2}{\sqrt{\eta(1-\eta)}} \left((1-\eta) \langle \hat{n}_{c_{(1)o}} \rangle - \eta \langle \hat{n}_{d_{(1)o}} \rangle - \frac{1-2\eta}{2} |\gamma|^2 \right) = \langle \gamma^* \hat{b} + \gamma \hat{b}^\dagger \rangle \quad (4.32)$$

from Eqs. (4.30) and (4.31). Thus, the expectation value of the self-adjoint operator $\gamma^*\hat{b} + \gamma\hat{b}^\dagger$ can be calculated through the photon number expectation value $\langle\hat{n}_{c(1)o}\rangle$ and $\langle\hat{n}_{d(1)o}\rangle$, if the non-vanishing complex amplitude γ of the coherent state from the local oscillator and the transmittance η of the beam splitter are also given.

The left-hand side of Eq. (4.32) is regarded as the expectation value of the operator \hat{s}_{D1D2} defined by

$$\hat{s}_{D1D2} := \frac{2}{\sqrt{\eta(1-\eta)}} \left((1-\eta)\hat{n}_{c(1)o} - \eta\hat{n}_{d(1)o} - \frac{1-2\eta}{2}|\gamma|^2 \right). \quad (4.33)$$

Through Eqs. (4.27), (4.28) and (4.29), in terms of the quadrature \hat{b} , \hat{l}_i , \hat{e}_i , and \hat{f}_i , the operator \hat{s}_{D1D2} defined by Eq. (4.33) is also expressed as

$$\begin{aligned} \hat{s}_{D1D2} = & \hat{b}\hat{l}_i^\dagger + \hat{b}^\dagger\hat{l}_i + \frac{1-2\eta}{\sqrt{\eta(1-\eta)}} \left(\hat{l}_i^\dagger\hat{l}_i - |\gamma|^2 \right) \\ & - \hat{b}\hat{f}_i^\dagger - \hat{b}^\dagger\hat{f}_i + \hat{e}_i\hat{f}_i^\dagger + \hat{e}_i^\dagger\hat{f}_i - \hat{e}_i\hat{l}_i^\dagger - \hat{e}_i^\dagger\hat{l}_i \\ & + \frac{1-2\eta}{\sqrt{\eta(1-\eta)}} \left(\hat{f}_i^\dagger\hat{f}_i - \hat{f}_i^\dagger\hat{l}_i - \hat{l}_i^\dagger\hat{f}_i \right). \end{aligned} \quad (4.34)$$

In the right-hand side of Eq. (4.34), the first line gives the expectation value (4.32), the second-line is the contributions from the vacuum inputs, and the final line is the vacuum contribution due to the unbalance of the beam splitter BS2.

5. Balanced homodyne detection through BS4

Next, we consider the balanced homodyne detection through the beam splitter BS4. Here, we again assume that the transmittance of the beamsplitter BS4 is η , as a simple model of the imperfections of the interferometer configurations. The important incident fields to the beam splitter BS4 is $\hat{b}_{(2)}$ and $\hat{l}_{(1/4)i}$ and the important outgoing fields from BS4 is $\hat{c}_{(2)o}$ and $\hat{d}_{(2)o}$. At the BS4, these fields are related as

$$\hat{c}_{(2)o} = \sqrt{\eta}\hat{l}_{(1/4)i} - \sqrt{1-\eta}\hat{b}_{(2)}, \quad \hat{d}_{(2)o} = \sqrt{\eta}\hat{b}_{(2)} + \sqrt{1-\eta}\hat{l}_{(1/4)i}. \quad (4.35)$$

Here, we consider the case where the transmittance of the beam splitter BS4 is also η , which equal to the transmittance of the beam splitter BS2, as a simple model of imperfections of the interferometer setup.

The quadrature $\hat{b}_{(2)}$ is related to the direct output quadrature \hat{b} through the second equation in Eqs. (4.22). On the other hand, the quadrature $\hat{l}_{(1/4)i}$ is related to the quadrature \hat{l}_i of the incident field from the local oscillator through the second equation of Eqs. (4.23) and the effect of the phase rotator (4.25). Then, Eqs. (4.35) are given by

$$\hat{c}_{(2)o} = \frac{1}{\sqrt{2}} \left(i\sqrt{\eta}\hat{l}_i - \sqrt{1-\eta}\hat{b} \right) + \frac{1}{\sqrt{2}} \left(i\sqrt{\eta}\hat{f}_i - \sqrt{1-\eta}\hat{e}_i \right), \quad (4.36)$$

$$\hat{d}_{(2)o} = \frac{1}{\sqrt{2}} \left(\sqrt{\eta}\hat{b} + i\sqrt{1-\eta}\hat{l}_i \right) + \frac{1}{\sqrt{2}} \left(\sqrt{\eta}\hat{e}_i + i\sqrt{1-\eta}\hat{f}_i \right). \quad (4.37)$$

Here, we note that the second terms in Eqs. (4.36) and (4.37) are the contribution of the incident vacuum field due to the interferometer configuration depicted in Fig. 3., respectively.

The photon numbers of the output fields associated with the quadratures $\hat{c}_{(2)o}$ and $\hat{d}_{(2)o}$ are detected through the photodetector D3 and D4 in Fig. 3, respectively. These photon-number operators are defined by

$$\hat{n}_{c(2)o} := \hat{c}_{(2)o}^\dagger\hat{c}_{(2)o}, \quad \hat{n}_{d(2)o} := \hat{d}_{(2)o}^\dagger\hat{d}_{(2)o}. \quad (4.38)$$

Through Eqs. (4.36) and (4.37), these operators are given in terms of the quadratures \hat{b} , \hat{l}_i , \hat{e}_i and \hat{f}_i . The expectation value of the photon number operator $\hat{n}_{c(2)o}$, which is detected by the photodetector D3, is given by

$$\langle\hat{n}_{c(2)o}\rangle = \frac{\eta}{2}|\gamma|^2 + \frac{i\sqrt{\eta(1-\eta)}}{2} \langle\gamma^*\hat{b} - \gamma\hat{b}^\dagger\rangle + \frac{1-\eta}{2} \langle\hat{n}_b\rangle. \quad (4.39)$$

On the other hand, the expectation value of the photon number operator $\hat{n}_{d(2)o}$, which is detected by the photodetector D4, is given by

$$\langle\hat{n}_{d(2)o}\rangle = \frac{\eta}{2} \langle\hat{n}_b\rangle - \frac{i\sqrt{\eta(1-\eta)}}{2} \langle\gamma^*\hat{b} - \gamma\hat{b}^\dagger(\omega)\rangle + \frac{1-\eta}{2}|\gamma|^2. \quad (4.40)$$

In the derivation of Eqs. (4.39) and (4.40), we used the field associated with the quadrature \hat{l}_i is in the coherent state with the complex amplitude γ and the fields associated with the quadratures \hat{e}_i and \hat{f}_i are in vacua. As in the case of the conventional balanced homodyne detection in Sec. II C, we obtain

$$-\frac{2i}{\sqrt{\eta(1-\eta)}} \left(\eta \langle \hat{n}_{c(2)o} \rangle - (1-\eta) \langle \hat{n}_{d(2)o} \rangle + \frac{1-2\eta}{2} |\gamma|^2 \right) = \langle \gamma^* \hat{b} - \gamma \hat{b}^\dagger \rangle. \quad (4.41)$$

from Eqs. (4.39) and (4.40). Thus, the expectation value of the anti-self-adjoint operator $\gamma^* \hat{b} - \gamma \hat{b}^\dagger$ can be calculated through the photon number expectation value $\langle \hat{n}_{c(2)o} \rangle$ and $\langle \hat{n}_{d(2)o} \rangle$, if the complex amplitude γ of the coherent state from the local oscillator and the transmittance η of the beam splitters B2 and B4 are also given.

The left-hand side of Eq. (4.41) is regarded as the expectation value of the operator $\hat{s}_{D3D4}(\omega)$ defined by

$$\hat{s}_{D3D4} := \frac{2i}{\sqrt{\eta(1-\eta)}} \left((1-\eta) \hat{n}_{d(2)o} - \eta \hat{n}_{c(2)o} - \frac{1-2\eta}{2} |\gamma|^2 \right). \quad (4.42)$$

Through Eqs. (4.36), (4.37), and (4.38), in terms of the quadrature \hat{b} , \hat{l}_i , \hat{e}_i , and \hat{f}_i , the operator \hat{s}_{D3D4} defined by Eq. (4.42) is also expressed as

$$\begin{aligned} \hat{s}_{D3D4} = & \hat{l}_i^\dagger \hat{b} - \hat{b}^\dagger \hat{l}_i + \frac{i(1-2\eta)}{\sqrt{\eta(1-\eta)}} \left(\hat{l}_i^\dagger \hat{l}_i - |\gamma|^2 \right) \\ & - \hat{b}^\dagger \hat{f}_i + \hat{b} \hat{f}_i^\dagger + \hat{l}_i^\dagger \hat{e}_i + \hat{f}_i^\dagger \hat{e}_i - \hat{e}_i^\dagger \hat{l}_i - \hat{e}_i^\dagger \hat{f}_i \\ & + \frac{i(1-2\eta)}{\sqrt{\eta(1-\eta)}} \left(\hat{f}_i^\dagger \hat{l}_i + \hat{l}_i^\dagger \hat{f}_i + \hat{f}_i^\dagger \hat{f}_i \right). \end{aligned} \quad (4.43)$$

In the right-hand side of Eq. (4.43), the first line gives the expectation value (4.41), the second-line is the contributions from the vacuum inputs, and the final line is the vacuum contribution due to the unbalance of the beam splitter BS4.

C. Input vacuum to the main interferometer

Before going to the discussions on the measurements of the annihilation or creation operator itself, we discuss the dependence between the photon fields in the interferometer. The output operators (4.34) and (4.43) to measure the operator \hat{b} or \hat{b}^\dagger are described by the quadratures \hat{b} , \hat{l}_i , \hat{e}_i , and \hat{f}_i . As depicted in Fig. 3, \hat{e}_i , \hat{f}_i , and \hat{l}_i are quadratures of the independent fields. Then, we should regard that these operators commute with each other:

$$[\hat{e}_i, \hat{f}_i] = [\hat{e}_i, \hat{f}_i^\dagger] = [\hat{f}_i, \hat{l}_i] = [\hat{f}_i, \hat{l}_i^\dagger] = [\hat{l}_i, \hat{e}_i] = [\hat{l}_i, \hat{e}_i^\dagger] = 0. \quad (4.44)$$

The main problem is whether or not we may regard the output quadrature \hat{b} is also independent of \hat{e}_i , \hat{f}_i , and \hat{l}_i . This is the point to be checked in this subsection.

To check the independence of the quadrature \hat{b} of the other quadratures, we have to remind that the operator \hat{b} is the output quadrature from the main interferometer. On the other hand, we have the input quadrature \hat{a} to the main interferometer. In general, the output quadrature \hat{b} may depend on the input quadrature \hat{a} . In many situation, we regard that the field associated with the quadrature \hat{a} is in vacuum. Here, we check this vacuum state for the quadrature \hat{a} is an independent vacuum from the states of the photon fields associated with the quadratures \hat{e}_i , \hat{f}_i , and \hat{l}_i through the interferometer configuration depicted in Fig. 3.

At the BS1, the quadrature \hat{a} is given by

$$\hat{a} = \frac{1}{\sqrt{2}} (\hat{a}_{(1)} + \hat{a}_{(2)}), \quad (4.45)$$

and, at the BS2, the quadrature $\hat{a}_{(1)}$ is given by

$$\hat{a}_{(1)} = \sqrt{\eta} \hat{c}_{(1)i} - \sqrt{1-\eta} \hat{d}_{(1)i}. \quad (4.46)$$

The quadratures $\hat{c}_{(1)i}$ and $\hat{d}_{(1)i}$ are the quadratures of the incident fields from detectors D1 and D2 to the BS2, respectively. On the other hand, through the junction at the BS4, the quadrature $\hat{a}_{(2)}$ is given by

$$\hat{a}_{(2)} = \sqrt{\eta} \hat{d}_{(2)i} - \sqrt{1-\eta} \hat{c}_{(2)i}. \quad (4.47)$$

The quadratures $\hat{c}_{(2)i}$ and $\hat{d}_{(2)i}$ are the quadratures of the incident fields from detectors D3 and D4 to the BS4, respectively.

Substituting Eqs. (4.46) and (4.47) into Eq. (4.45), we obtain

$$\hat{a} = \sqrt{\frac{\eta}{2}} (\hat{c}_{(1)i} + \hat{d}_{(2)i}) - \sqrt{\frac{1-\eta}{2}} (\hat{d}_{(1)i} + \hat{c}_{(2)i}). \quad (4.48)$$

We assume that the states associated with the quadratures $\hat{c}_{(1)i}$, $\hat{c}_{(2)i}$, $\hat{d}_{(1)i}$, and $\hat{d}_{(2)i}$ from the detectors D1, D3, D2, and D4 are vacua. Due to this situation, the state associated with the input quadrature \hat{a} is regarded as a vacuum. Furthermore, Eq. (4.48) indicates that the quadrature \hat{a} is independent of the quadratures \hat{e}_i , \hat{f}_i , and \hat{l}_i . Therefore, we may regard that

$$[\hat{a}, \hat{e}_i] = [\hat{a}, \hat{e}_i^\dagger] = [\hat{a}, \hat{f}_i] = [\hat{a}, \hat{f}_i^\dagger] = [\hat{a}, \hat{l}_i] = [\hat{a}, \hat{l}_i^\dagger] = 0, \quad (4.49)$$

and then, we may regard that

$$[\hat{b}, \hat{e}_i] = [\hat{b}, \hat{e}_i^\dagger] = [\hat{b}, \hat{f}_i] = [\hat{b}, \hat{f}_i^\dagger] = [\hat{b}, \hat{l}_i] = [\hat{b}, \hat{l}_i^\dagger] = 0. \quad (4.50)$$

This is the result to be checked in this subsection.

We use the commutation relations (4.44) and (4.50) when we evaluate the fluctuations in the measurements discussed in Sec. IV D and Sec. IV E.

D. Measurements of an annihilation operator \hat{b} and a creation operator \hat{b}^\dagger

In Sec. IV B, the expectation value of the operators \hat{s}_{D1D2} and \hat{s}_{D3D4} can be measure through the photon number expectation value at the photodetectors D1, D2, D3, and D4. In this subsection, we note that we can calculate the expectation values of the annihilation and creation operators of photon field from the expectation values of these operators. The simplified version of the ingredients of this subsection is already explained in Ref. [26]. However, this subsection includes additional explanations which is not described in Ref. [26].

Note that the field associated with the quadrature \hat{l}_i is in the coherent state with the complex amplitude γ and the fields associated with the quadratures \hat{f}_i and \hat{e}_i are in their vacuum states in the derivation of the form of the operators \hat{s}_{D1D2} and \hat{s}_{D3D4} . From their constructions, it is trivial that the expectation values of the operators \hat{s}_{D1D2} and \hat{s}_{D3D4} are given by

$$\langle \hat{s}_{D1D2} \rangle = \gamma^* \langle \hat{b} \rangle + \gamma \langle \hat{b}^\dagger \rangle, \quad \langle \hat{s}_{D3D4} \rangle = \gamma^* \langle \hat{b} \rangle - \gamma \langle \hat{b}^\dagger \rangle. \quad (4.51)$$

From these relation of the expectation value, we can easily obtain

$$\frac{1}{2\gamma^*} (\langle \hat{s}_{D1D2} \rangle + \langle \hat{s}_{D3D4} \rangle) = \langle \hat{b} \rangle, \quad (4.52)$$

$$\frac{1}{2\gamma} (\langle \hat{s}_{D1D2} \rangle - \langle \hat{s}_{D3D4} \rangle) = \langle \hat{b}^\dagger \rangle. \quad (4.53)$$

These are assertions which is pointed out in Ref. [26] and are trivial result from the construction of the operators \hat{s}_{D1D2} and \hat{s}_{D3D4} . However, we have to emphasize that the expectation values of the operators \hat{s}_{D1D2} and \hat{s}_{D3D4} are calculable through the expectation values of photon number operators which are measured at the photodetector D1, D2, D3, and D4, the complex amplitude γ for the coherent state from the local oscillator, and the transmittance η of the beam splitters B2 and B4. A similar assertion was also reported in Ref. [27] in the context of the nonclassicality criteria in terms of moments.

Here, we also note that the direct calculation from Eqs. (4.34) and (4.43) yields

$$\begin{aligned} \hat{t}_{b+} &:= \frac{1}{2\gamma^*} (\hat{s}_{D1D2} + \hat{s}_{D3D4}) \\ &= \hat{b} \frac{\hat{l}_i^\dagger}{\gamma^*} + \frac{(1+i)(1-2\eta)}{2\sqrt{\eta(1-\eta)}} \gamma \left(\frac{\hat{l}_i^\dagger \hat{l}_i}{|\gamma|^2} - 1 \right) \\ &\quad + \frac{1}{\gamma^*} \left(-\hat{b}^\dagger \hat{f}_i + \hat{e}_i \hat{f}_i^\dagger - \hat{e}_i^\dagger \hat{l}_i \right) \\ &\quad + \frac{(1+i)(1-2\eta)}{2\sqrt{\eta(1-\eta)}\gamma^*} \left(+i \hat{f}_i^\dagger \hat{f}_i - \hat{f}_i^\dagger \hat{l}_i - \hat{l}_i^\dagger \hat{f}_i \right). \end{aligned} \quad (4.54)$$

and

$$\begin{aligned}
\hat{t}_{b-} &:= \frac{1}{2\gamma} (\hat{s}_{D1D2} - \hat{s}_{D3D4}) \\
&= \hat{b}^\dagger \frac{\hat{l}_i}{\gamma} + \frac{(1-i)(1-2\eta)}{2\sqrt{\eta(1-\eta)}} \gamma^* \left(\frac{\hat{l}_i^\dagger \hat{l}_i}{|\gamma|^2} - 1 \right) \\
&\quad + \frac{1}{\gamma} \left(-\hat{b} \hat{f}_i^\dagger + \hat{e}_i^\dagger \hat{f}_i - \hat{e}_i \hat{l}_i^\dagger \right) \\
&\quad + \frac{(1-i)(1-2\eta)}{2\sqrt{\eta(1-\eta)}\gamma} \left(-i \hat{f}_i^\dagger \hat{f}_i - \hat{l}_i^\dagger \hat{f}_i - \hat{f}_i^\dagger \hat{l}_i \right). \tag{4.55}
\end{aligned}$$

We also note that

$$\hat{t}_{b+}^\dagger = \hat{t}_{b-} \tag{4.56}$$

from the explicit expression (4.54) and (4.55).

Through the explicit expression of the operators (4.54) and (4.55), we evaluate the fluctuations in the measurement of the expectation values (4.52) and (4.53). Since the operators $\hat{t}_{b\pm}$ are not self-adjoint as in Eq. (4.56), there is no guiding principle to evaluate their fluctuations, in general. In this paper, we evaluate the fluctuations through the expectation value

$$\left\langle \frac{1}{2} \left(\hat{t}_{b\pm}(\omega) \hat{t}_{b\pm}^\dagger(\omega') + \hat{t}_{b\pm}^\dagger(\omega') \hat{t}_{b\pm}(\omega) \right) \right\rangle. \tag{4.57}$$

The evaluation through Eq. (4.57) is commonly used to evaluate spectral densities [12, 18]. Furthermore, the operator $\hat{t}_{b\pm}$ has the property (4.56), the expectation value Eq. (4.57) is evaluated as

$$\left\langle \frac{1}{2} \left(\hat{t}_{b\pm}(\omega) \hat{t}_{b\pm}^\dagger(\omega') + \hat{t}_{b\pm}^\dagger(\omega') \hat{t}_{b\pm}(\omega) \right) \right\rangle = \frac{1}{2} \left(\langle \hat{t}_{b\pm}(\omega) | \hat{t}_{b\mp}(\omega') \rangle + \langle \hat{t}_{b\mp}(\omega') | \hat{t}_{b\pm}(\omega) \rangle \right), \tag{4.58}$$

where we defined

$$| \hat{t}_{b\pm}(\omega) \rangle := \hat{t}_{b\pm}(\omega) | \psi \rangle. \tag{4.59}$$

Furthermore, we note that

$$\begin{aligned}
\hat{t}_{b+}(\omega') \hat{t}_{b+}^\dagger(\omega) + \hat{t}_{b+}^\dagger(\omega) \hat{t}_{b+}(\omega') &= \hat{t}_{b+}(\omega') \hat{t}_{b-}(\omega) + \hat{t}_{b-}(\omega) \hat{t}_{b+}(\omega') \\
&= \hat{t}_{b-}^\dagger(\omega') \hat{t}_{b-}(\omega) + \hat{t}_{b-}(\omega) \hat{t}_{b-}^\dagger(\omega'). \tag{4.60}
\end{aligned}$$

This implies that the fluctuations in the measurement of the operator \hat{t}_{b-} through Eq. (4.57) is given by the fluctuations in the measurement of the operator \hat{t}_{b-} through Eq. (4.57) and the replacement $\omega \leftrightarrow \omega'$. For this reason, we only show the results of the fluctuations in the measurement of the expectation value of the operator \hat{t}_{b+} :

$$\begin{aligned}
\frac{1}{2} \langle \hat{t}_{b+} \hat{t}_{b+}^\dagger + \hat{t}_{b+}^\dagger \hat{t}_{b+} \rangle &= \left\langle \frac{1}{2} \left(\hat{b}'^\dagger \hat{b} + \hat{b} \hat{b}'^\dagger \right) \right\rangle \\
&\quad + \left(\frac{\langle \hat{n}_b \rangle}{|\gamma|^2} + \frac{1}{2} \right) 2\pi\delta(\omega - \omega') \\
&\quad + \frac{1-2\eta}{4\sqrt{\eta(1-\eta)}|\gamma|^2} \left\langle \gamma^*(\gamma^*+1)\hat{b} + \gamma(\gamma+1)\hat{b}^\dagger \right\rangle 2\pi\delta(\omega - \omega') \\
&\quad + i \frac{1-2\eta}{4\sqrt{\eta(1-\eta)}|\gamma|^2} \left\langle \gamma^*(\gamma^*-1)\hat{b} - \gamma(\gamma-1)\hat{b}^\dagger \right\rangle 2\pi\delta(\omega - \omega') \\
&\quad + \frac{(1-2\eta)^2}{2\eta(1-\eta)} (1 + |\gamma|^2) 2\pi\delta(\omega - \omega'). \tag{4.61}
\end{aligned}$$

Here, we note that the second line of the light-hand side of Eq. (4.61) comes from the shot noise contribution of the additional input vacua in the interferometer and the remaining lines of the right-hand side is due to the imperfection of the beam splitters BS2 and BS4 from 50:50.

Since we are concentrating on the case where the operators $\hat{t}_{b\pm}$, \hat{b} , and \hat{b}^\dagger have the nontrivial expectation values $\langle \hat{t}_{b+} \rangle = \langle \hat{b} \rangle$ and $\langle \hat{t}_{b-} \rangle = \langle \hat{b}^\dagger \rangle$, Eq. (4.61) includes not only the information of the fluctuations but also the information of the correlation of these expectation values. Therefore, to consider the fluctuations in the measurements of $\hat{t}_{b\pm}$, we have to eliminate the information of the correlation of the expectation values $\langle \hat{t}_{b+} \rangle = \langle \hat{b} \rangle$ and $\langle \hat{t}_{b-} \rangle = \langle \hat{b}^\dagger \rangle$ from Eq. (4.61). Actually, if we define the noise operator $\hat{t}_{b\pm}^{(n)}$ and $\hat{b}^{(n)}$ so that

$$\hat{t}_{b+} =: \langle \hat{b} \rangle + \hat{t}_{b+}^{(n)}, \quad \langle \hat{t}_{b+}^{(n)} \rangle = 0, \quad (4.62)$$

$$\hat{t}_{b-} =: \langle \hat{b}^\dagger \rangle + \hat{t}_{b-}^{(n)}, \quad \langle \hat{t}_{b-}^{(n)} \rangle = 0, \quad (4.63)$$

$$\hat{b} =: \langle \hat{b} \rangle + \hat{b}^{(n)}, \quad \langle \hat{b}^{(n)} \rangle = 0, \quad (4.64)$$

the left-hand side of Eq. (4.61) and the first term in the right-hand side of Eq. (4.61) yield

$$\frac{1}{2} \langle \hat{t}_{b+} \hat{t}_{b+}^\dagger + \hat{t}_{b+}^\dagger \hat{t}_{b+} \rangle = \frac{1}{2} \langle \hat{t}_{b+}^{(n)} \hat{t}_{b+}^{(n)\dagger} + \hat{t}_{b+}^{(n)\dagger} \hat{t}_{b+}^{(n)} \rangle + \langle \hat{b}' \rangle^* \langle \hat{b} \rangle, \quad (4.65)$$

$$\frac{1}{2} \langle \hat{b} \hat{b}^\dagger + \hat{b}^\dagger \hat{b} \rangle = \frac{1}{2} \langle \hat{b}^{(n)} \hat{b}^{(n)\dagger} + \hat{b}^{(n)\dagger} \hat{b}^{(n)} \rangle + \langle \hat{b}' \rangle^* \langle \hat{b} \rangle. \quad (4.66)$$

In the right-hand side of Eqs. (4.65) and (4.66), the first terms corresponds to the noise correlation and the second terms are the correlations of the signal in the measurements of operators \hat{b} and \hat{b}^\dagger .

For the quantum operator \hat{Q} with its expectation value $\langle \hat{Q} \rangle = 0$, we introduce the noise spectral density as in Refs. [12, 18] by

$$\frac{1}{2} S_{\hat{Q}}(\omega) 2\pi\delta(\omega - \omega') := \frac{1}{2} \left(\hat{Q}(\omega) \hat{Q}^\dagger(\omega') + \hat{Q}^\dagger(\omega') \hat{Q}(\omega) \right). \quad (4.67)$$

Then, Eq. (4.61) yields the relation between the noise spectral densities as

$$\begin{aligned} S_{\hat{t}_{b+}^{(n)}}(\omega) &= S_{\hat{b}^{(n)}}(\omega) + \frac{2\langle \hat{n}_b \rangle}{|\gamma|^2} + 1 \\ &+ \frac{1 - 2\eta}{2\sqrt{\eta(1-\eta)}|\gamma|^2} \langle \gamma^*(\gamma^* + 1)\hat{b} + \gamma(\gamma + 1)\hat{b}^\dagger \rangle \\ &+ i \frac{1 - 2\eta}{2\sqrt{\eta(1-\eta)}|\gamma|^2} \langle \gamma^*(\gamma^* - 1)\hat{b} - \gamma(\gamma - 1)\hat{b}^\dagger \rangle \\ &+ \frac{(1 - 2\eta)^2}{\eta(1-\eta)} (1 + |\gamma|^2). \end{aligned} \quad (4.68)$$

In the case where the beam splitters BS2 and BS4 is 50:50, i.e., $\eta = 1/2$, equation (4.68) gives

$$S_{\hat{t}_{b+}^{(n)}}(\omega) = S_{\hat{b}^{(n)}}(\omega) + \frac{2}{|\gamma|^2} \langle \hat{n}_b \rangle + 1. \quad (4.69)$$

This is the result which was shown in Ref. [26]. Equation (4.69) indicates that in addition to the noise spectral density $S_{\hat{b}^{(n)}}(\omega)$, we have the additional fluctuations which described by $2\langle \hat{n}_b \rangle/|\gamma|^2 + 1$ in the double balanced homodyne detection to measure \hat{b} through the measurement of \hat{t}_{b+} . We note that the term $2\langle \hat{n}_b \rangle/|\gamma|^2$ will be negligible if the absolute value of the complex amplitude γ is much larger than the expectation value of the output photon number $\langle \hat{n}_b \rangle$, i.e., $\langle \hat{n}_b \rangle \ll |\gamma|^2$. On the other hand, the term 1 in $2\langle \hat{n}_b \rangle/|\gamma|^2 + 1$, which is comes from the shot noise from the additional input vacuum fields in the interferometer for the double balanced homodyne detection, is not controllable.

E. Double balanced homodyne detection in two-photon description

Here, we consider the two-photon description, which is used in gravitational-wave community and show that we can calculate the expectation value $\langle \cos\theta\hat{b}_1 + \sin\theta\hat{b}_2 \rangle$ through the interferometer setup depicted in Fig. 3.

As discussed in Sec. III, in the two-photon formulation, we consider the sideband with the frequencies $\omega_0 \pm \Omega$ and we denote $\hat{b}(\omega_0 \pm \Omega) = \hat{b}_\pm$. The output through homodyne detection using D1 and D2 has the information of the

operators $\hat{s}_{D1D2}(\omega_0 \pm \Omega) = \hat{s}_{D1D2\pm}$, which are given by

$$\begin{aligned} \hat{s}_{D1D2\pm} &= \hat{b}_\pm \hat{l}_{i\pm}^\dagger + \hat{b}_\pm^\dagger \hat{l}_{i\pm} + \frac{1-2\eta}{\sqrt{\eta(1-\eta)}} \left(\hat{l}_{i\pm}^\dagger \hat{l}_{i\pm} - |\gamma_\pm|^2 \right) \\ &\quad - \hat{b}_\pm \hat{f}_{i\pm}^\dagger - \hat{b}_\pm^\dagger \hat{f}_{i\pm} + \hat{e}_{i\pm} \hat{f}_{i\pm}^\dagger + \hat{e}_{i\pm}^\dagger \hat{f}_{i\pm} - \hat{e}_{i\pm} \hat{l}_{i\pm}^\dagger - \hat{e}_{i\pm}^\dagger \hat{l}_{i\pm} \\ &\quad + \frac{1-2\eta}{\sqrt{\eta(1-\eta)}} \left(\hat{f}_{i\pm}^\dagger \hat{f}_{i\pm} - \hat{f}_{i\pm}^\dagger \hat{l}_{i\pm} - \hat{l}_{i\pm}^\dagger \hat{f}_{i\pm} \right) \end{aligned} \quad (4.70)$$

from Eq. (4.34). Following the discussion in Sec. IV A 2, we introduce the operators \hat{t}_{D1D2+} defined by

$$\hat{t}_{D1D2+} := \frac{1}{\sqrt{2}} \left(\frac{\hat{s}_{D1D2+}}{|\gamma_+|} + \frac{\hat{s}_{D1D2-}}{|\gamma_-|} \right), \quad (4.71)$$

where the electric field associated with the quadratures $\hat{l}_{i\pm}$ are in the coherent state with the complex amplitude γ_\pm and the phase θ_\pm of the complex amplitude γ_\pm is chosen so that

$$\theta_\pm = \theta. \quad (4.72)$$

This choice is an essential requirement for the measurement of the expectation value $\langle \cos \theta \hat{b}_1 + \sin \theta \hat{b}_2 \rangle$. Further, we also assume that

$$|\gamma_+| = |\gamma_-| =: |\gamma| \quad (4.73)$$

for simplicity. This assumption is easily generalized to the case $|\gamma_+| \neq |\gamma_-|$ as seen in Appendix A. Under this situation, we evaluate the operator \hat{t}_{D1D2+} defined by Eqs. (4.71). Substituting Eqs. (4.70) into Eq. (4.71) and using the definitions (3.5) of the operators \hat{b}_1 and \hat{b}_2 , we obtain

$$\begin{aligned} \hat{t}_{D1D2+} &= \frac{1}{2|\gamma|} \left(\hat{l}_{i-} + \hat{l}_{i+}^\dagger \right) \hat{b}_1 + \frac{1}{2i|\gamma|} \left(\hat{l}_{i-} - \hat{l}_{i+}^\dagger \right) \hat{b}_2 \\ &\quad + \frac{1}{2|\gamma|} \left(\hat{l}_{i+} + \hat{l}_{i-}^\dagger \right) \hat{b}_1^\dagger + \frac{1}{2i|\gamma|} \left(\hat{l}_{i+} - \hat{l}_{i-}^\dagger \right) \hat{b}_2^\dagger \\ &\quad + \frac{1-2\eta}{\sqrt{2\eta(1-\eta)}|\gamma|} \left(\hat{l}_{i+}^\dagger \hat{l}_{i+} + \hat{l}_{i-}^\dagger \hat{l}_{i-} - 2|\gamma|^2 \right) \\ &\quad + \frac{1}{\sqrt{2}|\gamma|} \left(-\hat{b}_+ \hat{f}_{i+}^\dagger - \hat{b}_+^\dagger \hat{f}_{i+} + \hat{e}_{i+} \hat{f}_{i+}^\dagger + \hat{e}_{i+}^\dagger \hat{f}_{i+} - \hat{e}_{i+} \hat{l}_{i+}^\dagger - \hat{e}_{i+}^\dagger \hat{l}_{i+} \right) \\ &\quad + \frac{1}{\sqrt{2}|\gamma|} \left(-\hat{b}_- \hat{f}_{i-}^\dagger - \hat{b}_-^\dagger \hat{f}_{i-} + \hat{e}_{i-} \hat{f}_{i-}^\dagger + \hat{e}_{i-}^\dagger \hat{f}_{i-} - \hat{e}_{i-} \hat{l}_{i-}^\dagger - \hat{e}_{i-}^\dagger \hat{l}_{i-} \right) \\ &\quad + \frac{1-2\eta}{\sqrt{2\eta(1-\eta)}} \frac{1}{|\gamma|} \left(\hat{f}_{i+}^\dagger \hat{f}_{i+} - \hat{f}_{i+}^\dagger \hat{l}_{i+} - \hat{l}_{i+}^\dagger \hat{f}_{i+} \right. \\ &\quad \quad \left. + \hat{f}_{i-}^\dagger \hat{f}_{i-} - \hat{f}_{i-}^\dagger \hat{l}_{i-} - \hat{l}_{i-}^\dagger \hat{f}_{i-} \right) \end{aligned} \quad (4.74)$$

From the construction of the operator \hat{t}_{D1D2+} , it is trivial that the expectation value of the operator (4.74) is given by

$$\langle \hat{t}_{D1D2+} \rangle = \langle \cos \theta \hat{b}_1 + \sin \theta \hat{b}_2 + \cos \theta \hat{b}_1^\dagger + \sin \theta \hat{b}_2^\dagger \rangle \quad (4.75)$$

On the other hand, the output through homodyne detection using D3 and D4 has the information of the operators $\hat{s}_{D3D4}(\omega_0 \pm \Omega) = \hat{s}_{D3D4\pm}$, which are given by

$$\begin{aligned} \hat{s}_{D3D4\pm} &= \hat{l}_{i\pm}^\dagger \hat{b}_\pm - \hat{b}_\pm^\dagger \hat{l}_{i\pm} + \frac{i(1-2\eta)}{\sqrt{\eta(1-\eta)}} \left(\hat{l}_{i\pm}^\dagger \hat{l}_{i\pm} - |\gamma_\pm|^2 \right) \\ &\quad - \hat{b}_\pm^\dagger \hat{f}_{i\pm} + \hat{b}_\pm \hat{f}_{i\pm}^\dagger + \hat{l}_{i\pm}^\dagger \hat{e}_{i\pm} + \hat{f}_{i\pm}^\dagger \hat{e}_{i\pm} - \hat{e}_{i\pm}^\dagger \hat{l}_{i\pm} - \hat{e}_{i\pm} \hat{f}_{i\pm}^\dagger \\ &\quad + \frac{i(1-2\eta)}{\sqrt{\eta(1-\eta)}} \left(\hat{f}_{i\pm}^\dagger \hat{l}_{i\pm} + \hat{l}_{i\pm}^\dagger \hat{f}_{i\pm} + \hat{f}_{i\pm}^\dagger \hat{f}_{i\pm} \right). \end{aligned} \quad (4.76)$$

from Eq. (4.43). Following the discussion in Sec. IV A 2, we introduce the operator \hat{t}_{D3D4-} defined by

$$\hat{t}_{D3D4-} := \frac{1}{\sqrt{2}} \left(\frac{\hat{s}_{D3D4+}}{|\gamma_+|} - \frac{\hat{s}_{D3D4-}}{|\gamma_-|} \right). \quad (4.77)$$

Under our situation where we assume Eqs. (4.72) and (4.73), the definition (4.77) is given by

$$\hat{t}_{D3D4-} := \frac{1}{\sqrt{2}|\gamma|} (\hat{s}_{D3D4+} - \hat{s}_{D3D4-}). \quad (4.78)$$

Substituting Eqs. (4.76) into Eq. (4.78) and using the definitions (3.5) of the operators \hat{b}_1 and \hat{b}_2 , we obtain

$$\begin{aligned} \hat{t}_{D3D4-} &= \frac{1}{2|\gamma|} (\hat{l}_{i-} + \hat{l}_{i+}^\dagger) \hat{b}_1 + \frac{1}{2i|\gamma|} (\hat{l}_{i-} - \hat{l}_{i+}^\dagger) \hat{b}_2 \\ &\quad - \frac{1}{2|\gamma|} (\hat{l}_{i+} + \hat{l}_{i-}^\dagger) \hat{b}_1^\dagger - \frac{1}{2i|\gamma|} (\hat{l}_{i+} - \hat{l}_{i-}^\dagger) \hat{b}_2^\dagger \\ &\quad + \frac{i(1-2\eta)}{|\gamma|\sqrt{2\eta(1-\eta)}} \left(+\hat{l}_{i+}^\dagger \hat{l}_{i+} - \hat{l}_{i-}^\dagger \hat{l}_{i-} \right) \\ &\quad + \frac{1}{\sqrt{2}|\gamma|} \left(-\hat{b}_+^\dagger \hat{f}_{i+} + \hat{b}_+ \hat{f}_{i+}^\dagger + \hat{l}_{i+}^\dagger \hat{e}_{i+} + \hat{f}_{i+}^\dagger \hat{e}_{i+} - \hat{e}_{i+}^\dagger \hat{l}_{i+} - \hat{e}_{i+}^\dagger \hat{f}_{i+} \right) \\ &\quad + \frac{1}{\sqrt{2}|\gamma|} \left(+\hat{b}_-^\dagger \hat{f}_{i-} - \hat{b}_- \hat{f}_{i-}^\dagger - \hat{l}_{i-}^\dagger \hat{e}_{i-} - \hat{f}_{i-}^\dagger \hat{e}_{i-} + \hat{e}_{i-}^\dagger \hat{l}_{i-} + \hat{e}_{i-}^\dagger \hat{f}_{i-} \right) \\ &\quad + \frac{i(1-2\eta)}{|\gamma|\sqrt{2\eta(1-\eta)}} \left(+\hat{f}_{i+}^\dagger \hat{l}_{i+} + \hat{l}_{i+}^\dagger \hat{f}_{i+} + \hat{f}_{i+}^\dagger \hat{f}_{i+} \right. \\ &\quad \quad \quad \left. - \hat{f}_{i-}^\dagger \hat{l}_{i-} - \hat{l}_{i-}^\dagger \hat{f}_{i-} - \hat{f}_{i-}^\dagger \hat{f}_{i-} \right). \end{aligned} \quad (4.79)$$

From the construction of the operator \hat{t}_{D3D4-} , it is trivial that the expectation value of the operator (4.79) is given by

$$\langle \hat{t}_{D3D4-} \rangle = \langle \cos \theta \hat{b}_1 + \sin \theta \hat{b}_2 - \cos \theta \hat{b}_1^\dagger - \sin \theta \hat{b}_2^\dagger \rangle. \quad (4.80)$$

From the expectation values (4.75) and (4.80), we obtain the expected result

$$\left\langle \frac{1}{2} (\hat{t}_{D1D2+} + \hat{t}_{D3D4-}) \right\rangle = \langle \cos \theta \hat{b}_1 + \sin \theta \hat{b}_2 \rangle \quad (4.81)$$

Thus, we have derived that the operator whose expectation value yields $\langle \cos \theta \hat{b}_1 + \sin \theta \hat{b}_2 \rangle$ is given by

$$\begin{aligned} \hat{t}_\theta &:= \frac{1}{2} (\hat{t}_{D1D2+} + \hat{t}_{D3D4-}) \\ &= \frac{1}{2\sqrt{2}|\gamma|} (\hat{s}_{D1D2+} + \hat{s}_{D1D2-} + \hat{s}_{D3D4+} - \hat{s}_{D3D4-}) \\ &= \frac{1}{2|\gamma|} (\hat{l}_{i-} + \hat{l}_{i+}^\dagger) \hat{b}_1 + \frac{1}{2i|\gamma|} (\hat{l}_{i-} - \hat{l}_{i+}^\dagger) \hat{b}_2 \\ &\quad + \frac{1-2\eta}{2\sqrt{2\eta(1-\eta)}|\gamma|} \left\{ (1+i)\hat{l}_{i+}^\dagger \hat{l}_{i+} + (1-i)\hat{l}_{i-}^\dagger \hat{l}_{i-} - 2|\gamma|^2 \right\} \\ &\quad + \frac{1}{\sqrt{2}|\gamma|} \left\{ -\hat{b}_+^\dagger \hat{f}_{i+} + \hat{e}_{i+} \hat{f}_{i+}^\dagger - \hat{e}_{i+}^\dagger \hat{l}_{i+} - \hat{b}_- \hat{f}_{i-}^\dagger - \hat{e}_{i-} \hat{l}_{i-}^\dagger + \hat{e}_{i-}^\dagger \hat{f}_{i-} \right\} \\ &\quad + \frac{(1+i)(1-2\eta)}{2\sqrt{2\eta(1-\eta)}|\gamma|} \left\{ \hat{f}_{i+}^\dagger \hat{f}_{i+} + i\hat{f}_{i+}^\dagger \hat{l}_{i+} + i\hat{l}_{i+}^\dagger \hat{f}_{i+} - i\hat{f}_{i-}^\dagger \hat{f}_{i-} \right. \\ &\quad \quad \quad \left. - \hat{f}_{i-}^\dagger \hat{l}_{i-} - \hat{l}_{i-}^\dagger \hat{f}_{i-} \right\}. \end{aligned} \quad (4.82)$$

As in the case of the measurement of $\langle \hat{b} \rangle$ or $\langle \hat{b}^\dagger \rangle$ in Sec. IV D, we evaluate the fluctuations in the measurement of the expectation value (4.81) through the explicit expression of the operators (4.82). We evaluate of the fluctuations

of the measurement of the operator \hat{t}_θ through the expectation value

$$\left\langle \frac{1}{2} \left(\hat{t}_\theta \hat{t}_\theta'^\dagger + \hat{t}_\theta'^\dagger \hat{t}_\theta \right) \right\rangle \quad (4.83)$$

as in the case of Sec. IV D, where we introduced the notation $\hat{Q}' := \hat{Q}(\Omega')$ for the frequency-dependent operator $\hat{Q} = \hat{Q}(\Omega)$. Tedious but straightforward calculations leads to the result

$$\begin{aligned} \left\langle \frac{1}{2} \left(\hat{t}_\theta \hat{t}_\theta'^\dagger + \hat{t}_\theta'^\dagger \hat{t}_\theta \right) \right\rangle &= \left\langle \frac{1}{2} \left(\hat{b}_\theta \hat{b}_\theta'^\dagger + \hat{b}_\theta'^\dagger \hat{b}_\theta \right) \right\rangle + \frac{1}{2} \left(1 + \frac{\langle \hat{n}_{b-} + \hat{n}_{b+} \rangle}{|\gamma|^2} \right) 2\pi\delta(\Omega - \Omega') \\ &+ \frac{1 - 2\eta}{2\sqrt{2\eta(1-\eta)}|\gamma|} \left\{ (\cos\theta - \sin\theta) \langle \hat{b}_1 + \hat{b}_1^\dagger \rangle \right. \\ &\quad \left. + (\cos\theta + \sin\theta) \langle \hat{b}_2 + \hat{b}_2^\dagger \rangle \right\} 2\pi\delta(\Omega - \Omega') \\ &+ \frac{(1 - 2\eta)^2}{\eta(1 - \eta)} 2\pi\delta(\Omega - \Omega'). \end{aligned} \quad (4.84)$$

where we denote $\hat{b}_\theta := \cos\theta\hat{b}_1 + \sin\theta\hat{b}_2$. The second term in the first line of the right-hand side of Eq. (4.84) comes from the shot noise contribution of the additional input vacua in the interferometer of the double balanced homodyne detection and the second-, third-, and fourth-lines of Eq. (4.84) is due to the imperfection of the beam splitters BS2 and BS4 from 50:50 as in the case of Sec. IV D.

The left-hand side and the first term in the right-hand side of Eq. (4.84) includes not only the information of the fluctuations in the measurement of the operator \hat{t}_θ , but also the information of the expectation value $\langle \hat{t}_\theta \rangle = \langle \hat{b}_\theta \rangle$. Therefore, we have to eliminate the information of the expectation value of the operator \hat{t}_θ from Eq. (4.84). To carry out this elimination, as in the case in Sec. IV D, we introduce the noise operators $\hat{t}_\theta^{(n)}$ and $\hat{b}_\theta^{(n)}$ by

$$\hat{t}_\theta =: \langle \hat{b}_\theta \rangle + \hat{t}_\theta^{(n)}, \quad \langle \hat{t}_\theta^{(n)} \rangle = 0, \quad (4.85)$$

$$\hat{b}_\theta =: \langle \hat{b}_\theta \rangle + \hat{b}_\theta^{(n)}, \quad \langle \hat{b}_\theta^{(n)} \rangle = 0. \quad (4.86)$$

In terms of these noise operators $\hat{t}_\theta^{(n)}$ and $\hat{b}_\theta^{(n)}$, the left-hand side of Eq. (4.84) is given by

$$\left\langle \frac{1}{2} \left(\hat{t}_\theta \hat{t}_\theta'^\dagger + \hat{t}_\theta'^\dagger \hat{t}_\theta \right) \right\rangle = \frac{1}{2} \left\langle \hat{t}_\theta^{(n)} \hat{t}_\theta^{(n)'\dagger} + \hat{t}_\theta^{(n)'\dagger} \hat{t}_\theta^{(n)} \right\rangle + \langle \hat{b}_\theta \rangle \langle \hat{b}_\theta' \rangle^*. \quad (4.87)$$

Similarly, the first term in the right-hand side of Eq. (4.84) is also given by

$$\frac{1}{2} \left\langle \hat{b}_\theta \hat{b}_\theta'^\dagger + \hat{b}_\theta'^\dagger \hat{b}_\theta \right\rangle = \frac{1}{2} \left\langle \hat{b}_\theta^{(n)} \hat{b}_\theta^{(n)'\dagger} + \hat{b}_\theta^{(n)'\dagger} \hat{b}_\theta^{(n)} \right\rangle + \langle \hat{b}_\theta \rangle \langle \hat{b}_\theta' \rangle^*. \quad (4.88)$$

In Eqs. (4.87) and (4.88), the first terms are corresponds to the noise correlation and the second term is the correlation of the expectation values.

Here, following Eq. (4.67), we introduce the noise spectral densities for the noise operators $\hat{t}_\theta^{(n)}$ and $\hat{b}_\theta^{(n)}$. Then, in terms of the noise spectral densities, Eq. (4.84) is given by

$$\begin{aligned} S_{\hat{t}_\theta^{(n)}}(\Omega) &= S_{\hat{b}_\theta^{(n)}}(\Omega) + \frac{\langle \hat{n}_{b-} + \hat{n}_{b+} \rangle}{|\gamma|^2} + 1 \\ &+ \frac{1 - 2\eta}{\sqrt{2\eta(1-\eta)}|\gamma|} \left\{ (\cos\theta - \sin\theta) \langle \hat{b}_1 + \hat{b}_1^\dagger \rangle + (\cos\theta + \sin\theta) \langle \hat{b}_2 + \hat{b}_2^\dagger \rangle \right\} \\ &+ \frac{(1 - 2\eta)^2}{2\eta(1 - \eta)}. \end{aligned} \quad (4.89)$$

In the case where the beam splitters BS2 and BS4 is 50:50, i.e., $\eta = 1/2$, equation (4.68) gives

$$S_{\hat{t}_\theta^{(n)}}(\Omega) = S_{\hat{b}_\theta^{(n)}}(\Omega) + \frac{\langle \hat{n}_{b-} + \hat{n}_{b+} \rangle}{|\gamma|^2} + 1. \quad (4.90)$$

As Eq. (4.69), equation (4.90) indicates that in addition to the spectral density $S_{\hat{b}_\theta}(\omega)$, we have the additional fluctuations which described by $\langle \hat{n}_{b+} + \hat{n}_{b-} \rangle / |\gamma|^2 + 1$ in the double balanced homodyne detection to measure the

expectation value of the operator \hat{b}_θ through the measurement of \hat{t}_θ . We note that the term $\langle \hat{n}_{b+} + \hat{n}_{b-} \rangle / |\gamma|^2$ will be negligible if the absolute value of the complex amplitude γ is much larger than the expectation value of the total output photon number $\langle \hat{n}_{b+} + \hat{n}_{b-} \rangle$ from the main interferometer as in the case of Sec. IV D. On the other hand, the term 1 in $2\langle \hat{n}_{b+} + \hat{n}_{b-} \rangle / |\gamma|^2 + 1$, which is comes from the shot noise from the additional input vacuum fields in the interferometer for the double balanced homodyne detection, is not controlable. This situation is same as that in Sec. IV D.

V. NOISE SPECTRUM OF THE GRAVITATIONAL-WAVE DETECTOR USING THE DOUBLE BALANCED HOMODYNE DETECTION

Here, we comment on the homodyne detection in gravitational-wave detectors. In this section, we concentrate only on the case $\eta = 1/2$, i.e., the transmittance of the beam splitters B2 and B4 is 50:50.

The input-output relation for the main interferometer to detect gravitational waves is formally given by Eq. (1.2), i.e.,

$$\hat{b}_\theta(\Omega) = R(\Omega) \left(\hat{h}_n(\Omega) + h(\Omega) \right), \quad (5.1)$$

where $h(\Omega)$ is the gravitational signal in the frequency domain which should be detected, $\hat{h}_n(\Omega)$ is the noise operator referred the gravitational-wave signal $h(\Omega)$ and $R(\Omega)$ is the response function of the detector. The gravitational-wave signal $h(\Omega)$ is classical which proportional to the identity operator in the sense of quantum theory. On the other hand, the noise operator $\hat{h}_n(\Omega)$ satisfies the property

$$\langle \hat{h}_n(\Omega) \rangle = 0. \quad (5.2)$$

Furthermore, the response function $R(\Omega)$ is a complex function.

Substituting Eq. (5.1) into the expression (4.81) of the expectation value \hat{t}_θ , we obtain

$$\langle \hat{t}_\theta(\Omega) \rangle = R(\Omega)h(\Omega). \quad (5.3)$$

where we used the definition (4.82) of the operator \hat{t}_θ and the property of the noise operator \hat{h}_n . Therefore, the expectation value of the operator $\langle \hat{t}_\theta(\Omega) \rangle / R(\Omega)$ yields the gravitational-wave signal $h(\Omega)$ in the frequency domain.

In the case of $h(\Omega) \neq 0$, the fluctuation directly evaluated through Eq. (4.83) also includes the information of the signal $h(\Omega)$ as in the case of Secs. IV D and IV E. This can be easily seen through Eq. (4.84) as

$$\begin{aligned} \left\langle \frac{1}{2} \left(\hat{t}_\theta \hat{t}_\theta'^\dagger + \hat{t}_\theta'^\dagger \hat{t}_\theta \right) \right\rangle &= R(\Omega)R^*(\Omega') \left\langle \frac{1}{2} \left(\hat{h}_n(\Omega)\hat{h}_n^\dagger(\Omega') + \hat{h}_n^\dagger(\Omega')\hat{h}_n(\Omega) \right) \right\rangle \\ &+ R(\Omega)R^*(\Omega')h^*(\Omega')h(\Omega) \\ &+ \frac{1}{2} \left(1 + \frac{\langle \hat{n}_{b-} + \hat{n}_{b+} \rangle}{|\gamma|^2} \right) 2\pi\delta(\Omega - \Omega'). \end{aligned} \quad (5.4)$$

The second-line of the right-hand side in Eq. (5.4) corresponds to the signal correlation. Since $\langle \hat{h}_n \rangle = 0$, we may apply the definition (4.67) of the noise spectral density. Then, we can easily obtain the definition of the signal referred noise spectral density in the measurement of the operator \hat{t}_θ as

$$\frac{1}{2R(\Omega)R^*(\Omega')} S_{\hat{t}_\theta^{(n)}}(\Omega) 2\pi\delta(\Omega - \Omega') := \left\langle \frac{1}{R(\Omega)R^*(\Omega')} \frac{1}{2} \left(\hat{t}_\theta \hat{t}_\theta'^\dagger + \hat{t}_\theta'^\dagger \hat{t}_\theta \right) \right\rangle - h^*(\Omega')h(\Omega). \quad (5.5)$$

We can also define the signal referred noise spectral density for the main interferometer as the noise spectral density for the operator \hat{h}_n through Eq. (4.67) :

$$\frac{1}{2} S_{\hat{h}_n}(\Omega) 2\pi\delta(\Omega - \Omega') := \left\langle \frac{1}{2} \left(\hat{h}_n(\Omega)\hat{h}_n^\dagger(\Omega') + \hat{h}_n^\dagger(\Omega')\hat{h}_n(\Omega) \right) \right\rangle. \quad (5.6)$$

Then, we obtain the relation of the noise spectral densities by

$$\frac{1}{|R(\Omega)|^2} S_{\hat{t}_\theta^{(n)}}(\Omega) = S_{\hat{h}_n}(\Omega) + \frac{1}{|R(\Omega)|^2} \left(1 + \frac{\langle \hat{n}_{b-}(\Omega) + \hat{n}_{b+}(\Omega) \rangle}{|\gamma(\Omega)|^2} \right). \quad (5.7)$$

It is reasonable to regard the noise spectral density (5.7) as the total signal referred noise spectral density through our double balanced homodyne detection in the situation where gravitational-wave signal exist.

From Eq. (5.7), we may say that in the situation $\langle \hat{n}_{b-}(\Omega) + \hat{n}_{b+}(\Omega) \rangle \ll |\gamma(\Omega)|^2$, the last term in the bracket of the second term of the right-hand side of Eq. (5.7) becomes harmless but the “1” of the first term in the same bracket cannot be controllable as in the cases of Secs. IV D and IV E. However, the situation of Eq. (5.7) is different from those in Secs. IV D and IV E. In Eq. (5.7), we have the response function in the front of the additional noise due to our double balanced homodyne detection. This implies that the signal referred noise spectral density (5.7) approaches to the signal referred noise spectral density $S_{\hat{h}_n}$ for the main interferometer in the situation where the response function $R(\Omega)$ is sufficient large.

VI. SUMMARY

As the summary of this paper, in Sec. II, we first reviewed the simple and the balanced homodyne detection through the understanding in the references [21, 22] to exclude ambiguities of understanding of “homodyne detections”. In this review, we use the Heisenberg picture in quantum theories and this picture enable us to make the explanations of the homodyne detections as compact as possible. This compact explanations of the homodyne detections enables us to consider more complicated interferometer setup. Although there are many researches on “homodyne detections”, we specify the basic understanding of the homodyne detection to avoid unnecessary confusions.

Based on this understanding of the homodyne detection, in Sec. III, we examine the balanced homodyne detection in the two-photon formulation [14]. The two-photon formulation is commonly used in the community of gravitational-wave detections. Our target in this paper is the statement in many papers, which states “*the measurement of the quadrature $\hat{b}_\theta := \cos\theta\hat{b}_1 + \sin\theta\hat{b}_2$ is carried out by the balanced homodyne detection [13].*” To examine whether or not this statement is correct, we consider the more precise statement, “the expectation value of the operator \hat{b}_θ can be measured as the linear combination of the upper- and lower-sidebands from the output of the balanced homodyne detection” and examined this statement. In this examination, we assume that the complex amplitude of the coherent state from the local oscillator is completely controllable. Our aim of this assumption is to find the requirements to the complex amplitude of the coherent state from the local oscillator.

Through this examination, we have reached to the conclusion that any linear combination of upper- and lower-sideband signal output of the balanced homodyne detection never yields the expectation value $\langle \hat{b}_\theta \rangle$. In this examination, we discuss more wider class of linear combinations of two quadratures, which are summarized in Table I. We considered six cases of linear combinations. Among them, two cases essentially include the situations where we can measure the expectation value \hat{b}_θ through the simple application of balanced homodyne detections. As seen in Table I, we found that many types of linear combinations of two quadratures which are essentially different from \hat{b}_θ is possible, but only two cases which include the situations of the measurement \hat{b}_θ is not possible. Therefore, the above statement “*the expectation value of the operator \hat{b}_θ can be measured as the linear combination of the upper- and lower-sidebands from the output of the balanced homodyne detection*” is incorrect.

Of course, in possible cases of Table I, we have been able to obtain the requirements to the complex amplitude of the coherent state from the local oscillator as expected. First, the complex amplitude of the coherent state from the local oscillator must have its support at the frequencies $\omega_0 \pm \Omega$. Second, the phase of the complex amplitude at the lower- and upper-sideband frequency must be chosen according to the possible cases as shown in Table I. The first requirement means that the complex amplitude of the coherent state from the local oscillator have its broad-band support. This will not be satisfied by the monochromatic laser sources. The second requirement for the phase of the complex amplitude is essential to obtain the desired output signals.

Through the understanding of the balanced homodyne detection based on Refs. [21, 22] and the examination in Sec. III, we reached to the proposal of the “*double balanced homodyne detection*” in Sec. IV. The application of this double balanced homodyne detection to the readout scheme enables us to measure the expectation values of the photon annihilation and creation operator themselves, which was reported in our previous letter [26]. The trivial extension of this double balanced homodyne detection to the two-photon formulation enables us to measure the above expectation value $\langle \hat{b}_\theta \rangle$, which cannot be measured through the simple application of the balanced homodyne detection as shown in Sec. III. The double balanced homodyne detection is the combination of two balanced homodyne detection whose phases of the complex amplitude of the coherent state from the local oscillator are different with $\pi/2$ from each other. Our theoretical idea of the double balanced homodyne detection comes from the examination in Sec. III. Through the examination in Sec. III, we found that if we can perform two balanced homodyne detection with the $\pi/2$ -phase different complex amplitudes of the coherent states from the local oscillator, we can measure the expectation values of the photon quadratures though these quadratures are not self-adjoint operators in quantum theory.

We also proposed the simple realization of our double balanced homodyne detection through the interferometer setup

in Sec. IV B. This interferometer setup is constructed by the taking into account of two balanced homodyne detections with the $\pi/2$ -phase difference in the complex amplitudes of the coherent states from the local oscillator. Then, in Sec. IV D, we showed that the interferometer setup proposed in Sec. IV B enables us to measure the expectation values of the annihilation and creation operators for the output photon field from the main interferometer. The interferometer setup for this double balanced homodyne detection is completely same as the eight-port homodyne detection in the literature [23–25] and we rediscovered this interferometer setup as the device to measure the expectation values of the photon creation and annihilation operators themselves. Furthermore, we also showed that the extension of our interferometer setup for the double balanced homodyne detection to the two-photon formulation enables us to measure the expectation value $\langle \hat{b}_\theta \rangle$. Thus, the correct statement is “*the expectation value of the operator $\hat{b}_\theta := \cos\theta\hat{b}_1 + \sin\theta\hat{b}_2$ can be measured as the linear combination of the upper- and lower-sidebands from the output of the double balanced homodyne detection.*”

We have to emphasize that our double balanced homodyne detection is not the direct measurement of the operator \hat{b}_θ . We just proposed the readout scheme which yields the expectation value $\langle \hat{b}_\theta \rangle$ through the four photon number measurements. The difference from the direct measurement of the operator \hat{b}_θ leads the additional fluctuations in the measurement, which also evaluated in Sec. IV E. To evaluate the noise in the measurement of the expectation value $\langle \hat{b}_\theta \rangle$, we also proposed an natural extension of the noise spectral density in the situation where the expectation value $\langle \hat{b}_\theta \rangle$ includes nontrivial information. We also discuss this extension of the evaluation of the noise spectral density in the case of gravitational-wave detections in Sec. V. As the result, we can concludes that the additional noise due to our double balanced homodyne detection can be negligible when the response function to the gravitational-wave signal of the gravitational-wave detector is sufficiently large.

As in the case of the examination in Sec. III, we found that there are requirements for the complex amplitude of the coherent state from the local oscillator also in the case of our double balanced homodyne detection in Sec. IV. First, the complex amplitude of the coherent state from the local oscillator must have its support at the upper- and lower-sideband frequencies $\omega_0 \pm \Omega$. Second, the phase θ_\pm of the complex amplitude of the coherent state from the local oscillator at the upper- and lower-sideband frequencies must be equal, i.e., $\theta_+ = \theta_-$.

In many literature, the optical field from the local oscillator is produced from the optical field in the main interferometer. However, the optical field in the main interferometer of the gravitational wave detector is a monochromatic laser. The complex amplitude of this monochromatic laser is a δ -function whose support is restricted at the frequency ω_0 . This complex amplitude does not have its support at the upper- and lower-sideband frequencies $\omega_0 \pm \Omega$. This contradicts to the above requirement to the complex amplitude of the coherent state from the local oscillator. Therefore, the experimental setup in the many literature cannot achieve the balanced homodyne detection itself. Even in the case of our double balanced homodyne detection, the complex amplitude of the coherent state from the local oscillator must have its support at the upper- and lower-sideband frequencies. Therefore, if we want to measure the expectation value $\langle \hat{b}_\theta \rangle$, the optical field from the oscillator must be changed so that its complex amplitude has its support at the upper- and lower-sideband frequency $\omega_0 \pm \Omega$.

Even if we do not apply our double balanced homodyne detection, we can carry out the usual balanced homodyne detection. In this case, we cannot measure the expectation value $\langle \hat{b}_\theta \rangle$ but we can measure a linear combination of \hat{b}_1 and \hat{b}_1^\dagger , or a linear combination of \hat{b}_2 and \hat{b}_2^\dagger , as depicted in Table I in Sec. III. Even in this case, the above two requirements to the complex amplitude of the coherent state from the local oscillator are crucial. Therefore, the requirements to the complex amplitude of the coherent state from the local oscillator clarified in this paper are very important requirements not only for our double balanced homodyne detection but also for the usual balanced homodyne detection.

If the realization of the above requirements for the optical fields from the local oscillator are accomplished, the realization of our double balanced homodyne detection is straightforward. We hope that our double balanced homodyne detection is confirmed in actual experiments and is used as a readout scheme of future gravitational wave detectors.

Acknowledgments

K.N. acknowledges to Dr. Tomotada Akutsu and the other members of the gravitational-wave project office in NAOJ for their continuous encouragement to our research. K.N. appreciate Prof. Akio Hosoya, Prof. Izumi Tsutsui, and Dr. Hiroyuki Takahashi for their support and continuous encouragement. We also appreciate Prof. Werner Vogel for valuable information.

Appendix A: Derivations of Eqs. (4.9)

If we may use a similar way to those in Sec. IV A 1, we can show that the expectation value of the operator $\cos \theta \hat{b}_1 + \sin \theta \hat{b}_2$ is also possible as discussed in Sec. IV A 2. Here, we show the explicit derivation of the definitions (4.9) of the operators \hat{t}_+ and \hat{t}_- , respectively. This is the aim of this Appendix.

To reach to this aim, we return to Eq. (3.9) and we concentrate only on the case where the coefficients α and β are real. In this case, the linear combination (3.9) is written in the form

$$\alpha \langle \hat{s}_+ \rangle + \beta \langle \hat{s}_- \rangle = \frac{1}{\sqrt{2}} \left\langle \kappa \hat{b}_1 + \lambda \hat{b}_2 + \kappa^* \hat{b}_1^\dagger + \lambda^* \hat{b}_2^\dagger \right\rangle. \quad (\text{A1})$$

Here, we defined

$$\kappa := \alpha \gamma_+^* + \beta \gamma_-, \quad \lambda := i (\alpha \gamma_+^* - \beta \gamma_-). \quad (\text{A2})$$

Here, we denote γ_\pm as

$$\gamma_\pm =: |\gamma_\pm| e^{i\theta_\pm}. \quad (\text{A3})$$

In terms of $|\gamma_\pm|$, θ_\pm , α , and β , from Eqs. (A2), we obtain the expression of κ and λ as

$$\kappa =: |\kappa| e^{i\varphi_\kappa}, \quad \lambda =: |\lambda| e^{i\varphi_\lambda}, \quad (\text{A4})$$

where $|\kappa|$, φ_κ , $|\lambda|$, and φ_λ are given by

$$|\kappa| = [\alpha^2 |\gamma_+|^2 + \beta^2 |\gamma_-|^2 + 2\alpha\beta |\gamma_+| |\gamma_-| \cos(\theta_+ + \theta_-)]^{1/2}, \quad (\text{A5})$$

$$\tan \varphi_\kappa = \frac{-\alpha |\gamma_+| \sin \theta_+ + \beta |\gamma_-| \sin \theta_-}{\alpha |\gamma_+| \cos \theta_+ + \beta |\gamma_-| \cos \theta_-}, \quad (\text{A6})$$

$$|\lambda| = [\alpha^2 |\gamma_+|^2 + \beta^2 |\gamma_-|^2 - 2\alpha\beta |\gamma_+| |\gamma_-| \cos(\theta_+ + \theta_-)]^{1/2}, \quad (\text{A7})$$

$$\tan \varphi_\lambda = \frac{\alpha |\gamma_+| \cos \theta_+ - \beta |\gamma_-| \cos \theta_-}{\alpha |\gamma_+| \sin \theta_+ + \beta |\gamma_-| \sin \theta_-}. \quad (\text{A8})$$

As seen in Sec. IV A 1, we can expect that the information of Eq. (A1) with vanishing phase in some sense and the information of Eq. (A1) with $\pi/2$ -phase in some sense are necessary. Further we will be able to derive the expectation value $\langle \cos \theta \hat{b}_1 + \sin \theta \hat{b}_2 \rangle$ from these information. As our speculation, we consider the cases $\varphi_\kappa = \varphi_\lambda = 0$ and $\varphi_\kappa = \varphi_\lambda = \pi/2$, respectively. As the result, we will see that our speculation is justified.

1. $\varphi_\kappa = \varphi_\lambda = 0$ case

First, we consider the case where $\varphi_\kappa = \varphi_\lambda = 0$. From Eqs. (A6) and (A8), this case is characterized by the equations

$$-\alpha |\gamma_+| \sin \theta_+ + \beta |\gamma_-| \sin \theta_- = 0, \quad (\text{A9})$$

$$\alpha |\gamma_+| \cos \theta_+ - \beta |\gamma_-| \cos \theta_- = 0. \quad (\text{A10})$$

Here, we note that $\alpha |\gamma_+| \neq 0$ and $\beta |\gamma_-| \neq 0$. From Eqs. (A9) and (A10), we obtain

$$\beta = \alpha \frac{|\gamma_+| \sin \theta_+}{|\gamma_-| \sin \theta_-} = \alpha \frac{|\gamma_+| \cos \theta_+}{|\gamma_-| \cos \theta_-}. \quad (\text{A11})$$

The second equality in Eq. (A11) gives

$$\tan \theta_+ = \tan \theta_-. \quad (\text{A12})$$

As a solution to Eq. (A12), we may choose

$$\theta_+ = \theta_-. \quad (\text{A13})$$

In this choice, the first equality in Eq. (A11) yields

$$\beta = \alpha \frac{|\gamma_+|}{|\gamma_-|}. \quad (\text{A14})$$

Substituting and Eqs. (A13) and (A14) into Eqs. (A5) and (A7), we obtain

$$\kappa = 2\alpha|\gamma_+||\cos\theta_+|, \quad \lambda = 2\alpha|\gamma_+||\sin\theta_+|. \quad (\text{A15})$$

Furthermore, through Eqs. (A13), (A14), and (A15), the linear combination (A1) is given by

$$\frac{1}{\sqrt{2}} \left(\frac{\langle \hat{s}_+ \rangle}{|\gamma_+|} + \frac{\langle \hat{s}_- \rangle}{|\gamma_-|} \right) = \left\langle |\cos\theta_+| \left(\hat{b}_1 + \hat{b}_1^\dagger \right) + |\sin\theta_+| \left(\hat{b}_2 + \hat{b}_2^\dagger \right) \right\rangle. \quad (\text{A16})$$

This is the expected result and corresponds to Eq. (4.2) in Sec. IV A 1. Therefore, the half of our speculation was correct.

2. $\varphi_\kappa = \varphi_\lambda = \pi/2$ case

Next, we consider the case where $\varphi_\kappa = \varphi_\lambda = \pi/2$. From Eq. (A6) and (A8), this case is characterized by the equations as

$$\alpha|\gamma_+|\cos\theta_+ + \beta|\gamma_-|\cos\theta_- = 0, \quad (\text{A17})$$

$$\alpha|\gamma_+|\sin\theta_+ + \beta|\gamma_-|\sin\theta_- = 0. \quad (\text{A18})$$

Here, we also note that $\alpha|\gamma_+| \neq 0$ and $\beta|\gamma_-| \neq 0$. From Eqs. (A17) and (A18), we obtain

$$\beta = -\alpha \frac{|\gamma_+|\cos\theta_+}{|\gamma_-|\cos\theta_-} = -\alpha \frac{|\gamma_+|\sin\theta_+}{|\gamma_-|\sin\theta_-}. \quad (\text{A19})$$

The second equality in Eq. (A19) gives

$$\tan\theta_+ = \tan\theta_-. \quad (\text{A20})$$

As a solution to Eq. (A20), we may choose

$$\theta_- = \theta_+, \quad (\text{A21})$$

as in the case of $\varphi_\kappa = \varphi_\lambda = 0$ in Sec. A 1. In this choice, the first equality in Eq. (A19) yields

$$\beta = -\alpha \frac{|\gamma_+|}{|\gamma_-|}. \quad (\text{A22})$$

Substituting Eqs. (A21) and (A22) into Eqs. (A5) and (A7), we obtain

$$\kappa = 2i\alpha|\gamma_+||\sin\theta_+|, \quad \lambda = 2i\alpha|\gamma_+||\cos\theta_+|. \quad (\text{A23})$$

Furthermore, through Eqs. (A21), (A22), and (A23), the linear combination (A1) is given by

$$\frac{1}{\sqrt{2}i} \left(\frac{\langle \hat{s}_+ \rangle}{|\gamma_+|} - \frac{\langle \hat{s}_- \rangle}{|\gamma_-|} \right) = \left\langle |\sin\theta_+| \left(\hat{b}_1 - \hat{b}_1^\dagger \right) + |\cos\theta_+| \left(\hat{b}_2 - \hat{b}_2^\dagger \right) \right\rangle. \quad (\text{A24})$$

This is also the expected result and corresponds to Eq. (4.3) in Sec. IV A 1. Therefore, the remaining part of our speculation was correct.

3. To calculate $\cos \theta \hat{b}_1 + \sin \theta \hat{b}_2$

As derived in the previous subsections, we have seen that we can obtain Eq. (A16) or (A24) through the appropriate choice of the complex amplitude γ_{\pm} for the coherent state from the local oscillator. To obtain Eq. (A16) as a signal output, we have to choose the phase of γ_{\pm} as Eq. (A13) and have to take the linear combination with the coefficients (α, β) as Eq. (A14). On the other hand, to obtain Eq. (A24) as a signal output, we have to choose the phase of γ_{\pm} as Eq. (A21) and have to take the linear combination with the coefficients (α, β) as Eq. (A22). The conditions (A13) and (A21) are same. Although the choice of the coefficients (α, β) are easy in practice, it is necessary to satisfy $|\gamma_{\pm}| \neq 0$. Therefore, to accomplish Eq. (A16) or (A24) as a signal output, $|\gamma_{\pm}| \neq 0$ and $\theta_+ = \theta_-$ are regarded as the requirement for the complex amplitude γ_{\pm} for the coherent state from the local oscillator.

As in the cases in Sec. IV A 1, we assume that the expectation values (A16) and (A24) can be independently obtained as the signal output at the same time. This assumption can be realized through the interferometer configuration depicted in Fig. 3.

If we choose the phase of the complex amplitude γ_{\pm} so that $\theta_{\pm} = \theta$ for the signal output (A16) and choose $\theta_{\pm} = \theta + \pi/2$ for the signal output (A24), these signal outputs are given by

$$\frac{1}{\sqrt{2}} \left(\frac{\langle \hat{s}_+ \rangle}{|\gamma_+|} + \frac{\langle \hat{s}_- \rangle}{|\gamma_-|} \right) \Big|_{\theta_{\pm}=\theta} = \left\langle |\cos \theta| (\hat{b}_1 + \hat{b}_1^{\dagger}) + |\sin \theta| (\hat{b}_2 + \hat{b}_2^{\dagger}) \right\rangle, \quad (\text{A25})$$

$$\frac{1}{\sqrt{2}i} \left(\frac{\langle \hat{s}_+ \rangle}{|\gamma_+|} - \frac{\langle \hat{s}_- \rangle}{|\gamma_-|} \right) \Big|_{\theta_{\pm}=\pi/2+\theta} = \left\langle |\cos \theta| (\hat{b}_1 - \hat{b}_1^{\dagger}) + |\sin \theta| (\hat{b}_2 - \hat{b}_2^{\dagger}) \right\rangle. \quad (\text{A26})$$

From Eqs. (A25) and (A26), we obtain

$$\begin{aligned} & \frac{1}{2} \left\{ \frac{1}{\sqrt{2}} \left(\frac{\langle \hat{s}_+ \rangle}{|\gamma_+|} + \frac{\langle \hat{s}_- \rangle}{|\gamma_-|} \right) \Big|_{\theta_{\pm}=\theta} + n \frac{1}{\sqrt{2}i} \left(\frac{\langle \hat{s}_+ \rangle}{|\gamma_+|} - \frac{\langle \hat{s}_- \rangle}{|\gamma_-|} \right) \Big|_{\theta_{\pm}=\pi/2+\theta} \right\} \\ & = \left\langle |\cos \theta| \hat{b}_1 + |\sin \theta| \hat{b}_2 \right\rangle. \end{aligned} \quad (\text{A27})$$

The factors $|\cos \theta|$ and $|\sin \theta|$ in Eq. (A27) is naturally replaced by $\cos \theta$ and $\sin \theta$, respectively, in Sec. IV A 2. Thus, we can see that if the expectation values (A16) and (A24) can be independently obtained as the signal output at the same time. We can measure the expectation value $\langle \cos \theta \hat{b}_1 + \sin \theta \hat{b}_2 \rangle$.

Before closing this appendix, we emphasize that the operators

$$\frac{1}{\sqrt{2}} \left(\frac{\hat{s}_+}{|\gamma_+|} + \frac{\hat{s}_-}{|\gamma_-|} \right), \quad \frac{1}{\sqrt{2}i} \left(\frac{\hat{s}_+}{|\gamma_+|} - \frac{\hat{s}_-}{|\gamma_-|} \right) \quad (\text{A28})$$

play the most important role for the measurement of $\langle \cos \theta \hat{b}_1 + \sin \theta \hat{b}_2 \rangle$. Therefore, in the main text, we begin our discussion from the explicit form of these operators.

Appendix B: Phase rotation operator in quantum theory

In this section, we briefly describes properties of the phase rotation operator (4.24) in quantum theory. First, we note that the following commutation relation:

$$\begin{aligned} \left[\int_0^{+\infty} \frac{d\Omega'}{2\pi} \left(\tilde{l}_{(1)i+}^{\dagger} \hat{l}'_{(1)i+} + \tilde{l}_{(1)i-}^{\dagger} \hat{l}'_{(1)i-} \right), \hat{l}_{(1)i\pm} \right] &= \int_0^{+\infty} \frac{d\Omega'}{2\pi} \left[\tilde{l}_{(1)i\pm}^{\dagger}, \hat{l}_{(1)i\pm} \right] \hat{l}'_{(1)i\pm} \\ &= \int_0^{+\infty} \frac{d\Omega'}{2\pi} \{-2\pi \delta(\Omega - \Omega')\} \hat{l}'_{(1)i\pm} \\ &= -\hat{l}_{(1)i\pm} \end{aligned} \quad (\text{B1})$$

Here, we consider a one-parameter family $\hat{B}(\lambda)$ of operator defined by

$$\hat{B}(\lambda) := e^{\lambda \hat{A}} B e^{-\lambda \hat{A}}. \quad (\text{B2})$$

Note that

$$\frac{\partial}{\partial \lambda} \hat{B}(\lambda) \Big|_{\lambda=0} = [\hat{A}, \hat{B}] =: \text{ad}_{\hat{A}} \hat{B}. \quad (\text{B3})$$

We also define $\text{ad}_{\hat{A}}^n \hat{B}$ by the recursion relation

$$\text{ad}_{\hat{A}}^n \hat{B} := [\hat{A}, \text{ad}_{\hat{A}}^{n-1} \hat{B}]. \quad (\text{B4})$$

Then, we easily check the following formula

$$\left. \frac{\partial^n}{\partial \lambda^n} \hat{B}(\lambda) \right|_{\lambda=0} = [\hat{A}, \text{ad}_{\hat{A}}^{n-1} \hat{B}] = \text{ad}_{\hat{A}}^n \hat{B}. \quad (\text{B5})$$

Through the operator $\text{ad}_{\hat{A}}^n \hat{B}$, we can express the operator $\hat{B}(\lambda)$ as

$$\hat{B}(\lambda) = \sum_{n=0}^{\infty} \frac{1}{n!} \lambda^n \text{ad}_{\hat{A}}^n \hat{B}, \quad (\text{B6})$$

in general. In particular, when the operators \hat{A} and \hat{B} satisfy the commutation relation $[\hat{A}, \hat{B}] = -\hat{A}$, we easily check that

$$\text{ad}_{\hat{A}}^n \hat{B} = (-1)^n \hat{B}. \quad (\text{B7})$$

and

$$\hat{B}(\lambda) = \sum_{n=0}^{\infty} \frac{1}{n!} \lambda^n (-1)^n \hat{B} = e^{-\lambda} \hat{B}. \quad (\text{B8})$$

Since we have the commutation relation (B1), we can easily check that

$$R(\theta) \hat{l}_{(1)i\pm} R(\theta)^\dagger = e^{i\theta} \hat{l}_{(1)i\pm}. \quad (\text{B9})$$

where we used

$$R^\dagger(\theta) = R^{-1}(\theta) = R(-\theta). \quad (\text{B10})$$

The phase rotator (PR) in Fig. 3 is defined as a device which operates to the quadrature $\hat{l}_{(1)i}$ and produce the quantum field associated with the quadrature $\hat{l}_{(1/4)i}$ as the output field so that

$$\hat{l}_{(1/4)i} = R\left(\frac{\pi}{2}\right) \hat{l}_{(1)i} R^\dagger\left(\frac{\pi}{2}\right) = e^{i(\pi/2)} \hat{l}_{(1)i} = i \hat{l}_{(1)i} \quad (\text{B11})$$

-
- [1] J. Aasi et al., *Class. Quantum Grav.* **32** (2015), 074001.
[2] B. P. Abbot et al. (LIGO Scientific Collaboration and Virgo Collaboration), *Phys. Rev. Lett.* **116** (2016), 061102.
[3] B. P. Abbot et al. (LIGO Scientific Collaboration and Virgo Collaboration), *Phys. Rev. Lett.* **116** (2016), 241103.
[4] B. P. Abbot et al. (LIGO Scientific Collaboration and Virgo Collaboration), *Phys. Rev. D* **93** (2016), 122003; B. P. Abbot et al. (LIGO Scientific Collaboration and Virgo Collaboration), *Phys. Rev. X* **6** (2016), 041015.
[5] B. P. Abbot et al. (LIGO Scientific Collaboration and Virgo Collaboration), *Phys. Rev. Lett.* **118** (2017), 221101.
[6] B. P. Abbot et al. (LIGO Scientific Collaboration and Virgo Collaboration), *Phys. Rev. Lett.* **119** (2017), 141101.
[7] B. P. Abbot et al. (LIGO Scientific Collaboration and Virgo Collaboration), *Phys. Rev. Lett.* **119** (2017), 161101.
[8] B. P. Abbot et al. (LIGO Scientific Collaboration and Virgo Collaboration), *Astrophys. J. Lett.* **848** (2017), L12.
[9] F. Acernese et al., *Class. Quantum Grav.* **32** (2015), 024001.
[10] Y. Aso, Y. Michimura, K. Somiya, M. Ando, O. Miyakawa, T. Sekiguchi, D. Tatsumi, H. Yamamoto, *Phys. Rev. D* **88** (2013), 043007.
[11] See as a recent review of this topic: S. L. Danilishin and F. Y. Khalili, *Living Rev. of Relativ.* **15** (2012), 5.
[12] H. J. Kimble, Y. Levin, A. B. Matsko, K. S. Thorne, and S. P. Vyatchanin, *Phys. Rev. D* **65** (2001), 022002.
[13] S. P. Vyatchanin and A. B. Matsko, *JETP* **77** (1993), 218; S. P. Vyatchanin and E. A. Zubova, *Phys. Lett. A* **203** (1995), 269; S. P. Vyatchanin, *ibid.* **239** (1998), 201; S. P. Vyatchanin and A. B. Matsko, *JETP* **82** (1996), 1007; S. P. Vyatchanin and A. B. Matsko, *ibid.*, **83** (1996), 690.
[14] C. M. Caves, and B. L. Schumaker, *Phys. Rev. A* **31** (1985), 3068; *ibid.* **31** (1985), 3093.
[15] V. B. Braginsky, *JETP* **26** (1968), 831.

- [16] V. B. Braginsky and F. Y. Khalili, *Quantum Measurement* (Cambridge University Press, 1992).
- [17] C. Bond, D. Brown, A. Freise, and K. A. Strain, *Living Rev. Relativ.* **19** (2016), 1.
- [18] H. Miao, “Exploring Macroscopic Quantum Mechanics in Optomechanical Devices”, PhD. thesis, The University of Western Australia, 2010.
- [19] K. McKenzie, M. B. Gray, P. K. Lam, and D. E. McClelland, *Appl. Opt.* **46** (2007), 3389.
- [20] M. S. Stefszky, C. M. Mow-Lowry, S. S. Y Chua, D. A. Shaddock, B. C. Buchler, H. Vahlbruch, A. Khalaidovski, R. Schnabel, P. K. Lam, and D. E. McClelland, *Class. Quantum Grav.* **29** (2012), 145015.
- [21] H. M. Wiseman and G. J. Milburn, *Quantum Measurement and Control* (Cambridge, UK: Cambridge University Press, 2009).
- [22] H. M. Wiseman and G. J. Milburn, *Phys. Rev. A* **47** (1993), 642.
- [23] N. G. Walker and J. E. Carrol, *Opt. Quantum Electron.* **18** (1986), 355; N. G. Walker, *J. Mod. Opt.* **34** (1987), 15.
- [24] J. W. Noh, A. Fougères, and L. Mandel, *Phys. Rev. Lett.* **67** (1991), 1426; *Phys. Rev. A* **45** (1992), 424; *ibid.*, **46** (1992), 2840; *Phys. Rev. Lett.* **71** (1993), 2579.
- [25] M. G. Raymer, J. Cooper, and M. Beck, *Phys. Rev. A* **48** (1993), 4617.
- [26] K. Nakamura and M.-K. Fujimoto, arXiv:1709.01697.
- [27] E. Shchukin, Th. Richter, W. Vogel, *Phys. Rev. A* **71** (2005), 011802(R); E. V. Shchukin, W. Vogel, *Phys. Rev. A* **72** (2005), 043808.